Neurobiology of Disease 182 (2023) 106134

Contents lists available at ScienceDirect

Neurobiology of Disease

journal homepage: www.elsevier.com/locate/ynbdi

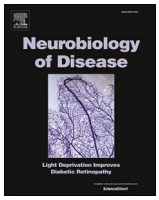

Decreased expression of synaptic genes in the vestibular ganglion of rodents following subchronic ototoxic stress.

Erin A. Greguske [a,b,c,1,2], Alberto F. Maroto [a,b,c,1], Mireia Borrajo [a,b,c], Aïda Palou [a,b,c], Marta Gut [d,e], Anna Esteve-Codina [d,e], Alejandro Barrallo-Gimeno [a,b,c], Jordi Llorens [a,b,c,*]

[a] Departament de Ciències Fisiològiques, Universitat de Barcelona, Feixa Llarga s/n, 08907 l'Hospitalet de Llobregat, Catalunya, Spain
[b] Institut de Neurociències, Universitat de Barcelona, Barcelona, Catalunya, Spain
[c] Institut d'Investigació Biomèdica de Bellvitge (IDIBELL), 08907 l'Hospitalet de Llobregat, Catalunya, Spain
[d] CNAG-CRG, Centre for Genomic Regulation, Barcelona Institute of Science and Technology (BIST), Barcelona, Spain
[e] Universitat Pompeu Fabra, Barcelona, Spain

ARTICLE INFO

Keywords:
Chronic vestibular toxicity
Ototoxicity
Vestibular ganglion neurons
Vestibular hair cells
RNA-seq
Synaptic uncoupling
BDNF
Nitrile ototoxicity
Rat
Mouse

ABSTRACT

The vestibular ganglion contains primary sensory neurons that are postsynaptic to the transducing hair cells (HC) and project to the central nervous system. Understanding the response of these neurons to HC stress or loss is of great interest as their survival and functional competence will determine the functional outcome of any intervention aiming at repair or regeneration of the HCs. We have shown that subchronic exposure to the ototoxicant 3,3′-iminodipropionitrile (IDPN) in rats and mice causes a reversible detachment and synaptic uncoupling between the HCs and the ganglion neurons. Here, we used this paradigm to study the global changes in gene expression in vestibular ganglia using RNA-seq. Comparative gene ontology and pathway analyses of the data from both model species indicated a robust downregulation of terms related to synapses, including presynaptic and postsynaptic functions. Manual analyses of the most significantly downregulated transcripts identified genes with expressions related to neuronal activity, modulators of neuronal excitability, and transcription factors and receptors that promote neurite growth and differentiation. For choice selected genes, the mRNA expression results were replicated by qRT-PCR, validated spatially by RNA-scope, or were demonstrated to be associated with decreased expression of the corresponding protein. We conjectured that decreased synaptic input or trophic support on the ganglion neurons from the HC was triggering these expression changes. To support this hypothesis, we demonstrated decreased expression of BDNF mRNA in the vestibular epithelium after subchronic ototoxicity and also downregulated expression of similarly identified genes (e.g *Etv5*, *Camk1g*, *Slc17a6*, *Nptx2*, *Spp1*) after HC ablation with another ototoxic compound, allylnitrile. We conclude that vestibular ganglion neurons respond to decreased input from HCs by decreasing the strength of all their synaptic contacts, both as postsynaptic and presynaptic players.

1. Introduction

The vestibular system in the inner ear is a sensor of head accelerations that encodes information for gaze control, equilibrium, motor control, and spatial orientation (Burns and Stone, 2017; Kandel et al., 2021; Elliott and Straka, 2022; Bacqué-Cazenave et al., 2022). In mammals, the sensory transducing cells of this system, named hair cells (HCs), are located in five sensory epithelia per ear: three cristae, one for each of the three semicircular canals, one macula in the utricle and one macula in the saccule. The HCs are presynaptic to vestibular ganglion neurons that project to the vestibular nuclei in the central nervous system. Stimuli cause changes in the amount of neurotransmitters released by the HC, thus modifying the frequency of action potentials fired by the ganglion neurons. Since both the HCs and the ganglion neurons are

Abbreviations: HC, hair cell; IDPN, 3,3′-iminodipropionitrile.

* Corresponding author at: Departament de Ciències Fisiològiques, Universitat de Barcelona, Feixa Llarga s/n, 08907 l'Hospitalet de Llobregat, Catalunya, Spain.
E-mail addresses: mborrajoarjona@ub.edu (M. Borrajo), apaloumi45@ub.edu (A. Palou), marta.gut@cnag.crg.eu (M. Gut), anna.esteve@cnag.crg.eu (A. Esteve-Codina), abarrallo@ub.edu (A. Barrallo-Gimeno), jllorens@ub.edu (J. Llorens).

[1] E.A.G. and A.F.M. contributed equally.
[2] Present address: Emulate, Inc., Boston, MA, USA.

https://doi.org/10.1016/j.nbd.2023.106134
Received 3 March 2023; Received in revised form 14 April 2023; Accepted 23 April 2023
Available online 24 April 2023

postmitotic and have little regeneration potential in most mammals, a loss of these cells results in an irreversible loss of function. This loss may occur due to genetic defects, aging, exposure to ototoxic compounds, and other damaging factors.

Recently, increasing evidence has shown that in addition to the loss of HCs or ganglion neurons, injuring stimuli may result in more subtle pathological effects that may exhibit different degrees of repair (Sedó-Cabezón et al., 2015; Gaboyard-Niay et al., 2016; Sultemeier and Hoffman, 2017; Greguske et al., 2019; Cassel et al., 2019; Kim et al., 2022; Maroto et al., 2022). Data from studies on chronic systemic exposure to ototoxic compounds (Sedó-Cabezón et al., 2015; Greguske et al., 2019; Maroto et al., 2022) indicate that HCs under stress trigger a reversible response of detachment from the postsynaptic neuron, resulting in the functional uncoupling of the synapse between these two cells. In these examples, the repair of the pathology associates with recovery of vestibular function. These damage and repair phenomena may explain, at least in part, clinical observations of functional recovery after ototoxicity caused by aminoglycoside antibiotics (Black et al., 2001), which are generally assumed to selectively target HCs (O'Sullivan et al., 2017; Kenyon et al., 2021). The role of synaptic pathology and repair in vestibular dysfunction and recovery has been only partially unveiled by these studies. More research is available on similar phenomena in the cochlea, where lack of synaptic recovery after a variety of insults, especially noise, has been demonstrated to be a major contributor to hearing loss (Liberman and Kujawa, 2017).

One important issue to understand is how vestibular ganglion neurons respond to the chronic HC stress induced by ototoxicants. While some of the major responses so far identified in the sensory epithelium occur in the neuron, such as the loss of the adhesion protein CASPR1 and of the postsynaptic components (GluA2 and PSD-95 puncta)(Sedó-Cabezón et al., 2015; Greguske et al., 2019; Maroto et al., 2022), its general response has not been investigated. Understanding the response of the ganglion neurons to insults primarily targeting the HCs is of paramount importance. First, the survival and adequate function of these neurons are necessary conditions for the success of any regeneration or replacement approach to treating HC loss. Second, because both decreased activity or loss of these neurons may have trans-synaptic impacts on the central nervous system. In this study, we evaluated whether a distinct gene expression response is triggered in the vestibular ganglion during the synaptic uncoupling associated with chronic ototoxicity. To this end, we used the subchronic 3,3′-iminodipropionitrile (IDPN) exposure model. As this model works well in rats (Sedó-Cabezón et al., 2015) and mice (Greguske et al., 2019), we studied both models to identify the more conserved responses across species, and would likely have a higher translational interest. The data obtained demonstrated a robust decrease in expression of synaptic protein genes in both species. In addition, we collected data demonstrating that this response is also triggered in the ganglion by the loss of synaptic input caused by HC ablation by a different ototoxin.

2. Materials and methods

2.1. Animals and treatments

Animals were used according to the Law 5/1995, Act 214/1997 of the Generalitat de Catalunya, and the 2010/63/UE directive, as approved by the University of Barcelona's Ethics Committee on Animal Experiments and the Commission on Animal Experimentation of the Generalitat (project numbers 265.19, 266.19 and 10,913). Young adult (8–9 weeks) Long-Evans rats were purchased from Janvier Labs (Le-Genest-Saint-Isle, France), acclimatized for at least 7 days before experimentation, housed two or three per cage, and given free access to drinking water and standard food pellets (TEKLAD 2014, Harlan Laboratories, Sant Feliu de Codines, Spain). We also used adult (2–5-month-old) 129S1/SvImJ mice from a local colony descendant of animals purchased from Jackson Laboratory (Bar Harbor, ME, USA). Only male animals were used because the outcome of the IDPN exposure model is different between sexes, likely due to differences in the metabolism of the xenobiotic, and males offer a better vestibular versus systemic toxicity ratio both in rats (Sedó-Cabezón et al., 2015) and mice (Greguske et al., 2019). These previous studies also demonstrated that substantial but still reversible loss of vestibular function, associated with synaptic uncoupling and little or no HC loss, can be elicited in both species using drinking water exposure to IDPN. However, different concentrations and times are needed to attain similar effects in either species. Accordingly, 0 or 20 mM of IDPN (>98%, TCI Europe, Zwijndrecht, Belgium) were added to the drinking water of the control (CTRL) and treated (IDPN) rats, respectively, for 4 weeks. Control and treated mice were exposed to 0 or 30 mM of IDPN in the drinking water, respectively, for 8 weeks.

Mice were also used to evaluate the impact of HC loss on gene expression. In this experiment, experimental animals were co-exposed to 1.2 mmol/kg of allylnitrile (>98%, Merck- Schuchard, Hohenbrunn bei München, Germany) and two doses of 100 mg/kg of *trans*-1,2-dichloroethylene (TDCE, 98%, Sigma-Aldrich, Madrid, Spain). Both compounds were administered p.o. in 6 ml/kg of corn oil. TDCE was given half an hour before and six hours after the allylnitrile dose. TDCE is an inhibitor of the CYP2E1 enzyme that reduces the systemic toxicity of allylnitrile and thus ameliorates the utility of this nitrile to cause HC loss (Saldaña-Ruíz et al., 2013). Half of the animals in the control group in this experiment received only the corn oil vehicle and the other half received corn oil and TDCE. Mice in this experiment were euthanized for sample collection three weeks after administration.

2.2. Evaluation of vestibular function

To ascertain that the animals used in the molecular analyses had the expected degree of loss of vestibular function, they were assessed at least once a week during or after treatment, and at the end of the experimental period. In mice, we obtained vestibular dysfunction ratings (VDRs), a semi-quantitative evaluation that uses a behavioural test battery. This battery includes 6 behaviours, both spontaneous and reflex, and rates each on a scale of 0–4 to yield a global VDR from 0 to 24. The VDRs offer a sensitive and specific measure of vestibular function loss and were obtained as described in detail elsewhere (Llorens et al., 1993; Soler-Martín et al., 2007; Saldaña-Ruíz et al., 2013; Greguske et al., 2019). In rats, we assessed the tail-lift reflex as described previously (Martins-Lopes et al., 2019; Maroto et al., 2021a, 2021b). The tail-lift reflex was also used to assess vestibular loss in the mice experiment evaluating the effect of HC loss in gene expression.

2.3. Sample collection and processing

For RNA studies, animals were decapitated, and their vestibular ganglia and epithelia were quickly dissected in ice-cold phosphate-buffered saline (PBS). The two ganglia from each animal were pooled in an Eppendorf tube, immediately frozen in liquid nitrogen, and stored at −80 °C until further processing. The sensory epithelia from the six cristae and two utricles from each animal were ripped off adjacent membranes and pooled, frozen, and stored similarly. RNA was extracted using the Qiagen RNeasy mini kit and protocol. Total RNA samples were quantified by Qubit® RNA BR Assay kit (Thermo Fisher Scientific, Waltham, MA, USA) and the RNA integrity was estimated with an Agilent RNA 6000 Pico Bioanalyzer 2100 Assay (Agilent Technologies, Santa Clara, CA, USA).

We also used samples available in the laboratory from previously reported experiments (Sedó-Cabezón et al., 2015; Greguske et al., 2019). These included ganglia from control and subchronic IDPN rats, treated as explained above, that had been fixed with 4% paraformaldehyde in PBS for 1 h and had been stored at −20 °C in a cryo-preservative solution (34.5% glycerol, 30% ethylene glycol, 20% PBS, 15.5% distilled water) for up to 10 years. For each analysis, we used ganglia from control and

treated animals that had been obtained at the same time. The specimens were rinsed of the cryopreservative solution in PBS, embedded in a block of agar, and sectioned at 30 μm in a vibrating microtome. The sections were processed for immunofluorescent expression studies and for RNAscope *in situ* hybridisation, as described below. We also used archival mouse ganglia that had been obtained and stored at −80 °C for RNA studies, as described above. These included samples from control mice, mice treated with IDPN for 8 weeks, and mice treated similarly but euthanized at the end of a washout period of 12 weeks following the exposure period. The number of animals and samples included in each experiment are provided in the Results section and detailed in Supplementary table S1.

2.4. Short read, low-input RNA sequencing

Two RNA-seq experiments (in rat and mouse animal models) were run, each comparing 3 control and 3 subchronic IDPN animals. RNA sequencing libraries were prepared following the SMARTseq2 protocol (Picelli et al., 2014) with some modifications. Briefly, reverse transcription of the total RNA input material of 1.8 μl (6–11 ng, in function of the sample availability) was performed using SuperScript II (Invitrogen) in the presence of oligo-dT30VN (1 μM; 5′-AAG CAG TGG TAT CAA CGC AGA GTA CT30VN-3′), template-switching oligonucleotides (1 μM) and betaine (1 M). The cDNA was amplified using the KAPA Hifi Hotstart ReadyMix (2×) (Roche) and 100 nM IS PCR primer (5′-AAG CAG TGG TAT CAA CGC AGA GT-3′) with 8 cycles of PCR amplification. Following purification with Agencourt Ampure XP beads (1:1 ratio; Beckmann Coulter), the product size distribution and the quantity were assessed with a Bioanalyzer High Sensitivity DNA Kit (Agilent). The amplified cDNA (200 ng) was fragmented for 10 min at 55 °C using Nextera XT (Illumina) and amplified for 12 cycles with indexed Nextera PCR primers. The library was purified twice with Agencourt Ampure XP beads (0.8:1 ratio) and quantified on a Bioanalyzer using a High Sensitivity DNA Kit.

The libraries were sequenced on HiSeq2000 (Illumina) in paired-end mode with a read length of 2x76bp using TruSeq SBS Kit v3-HS (Illumina) in a fraction of a sequencing flow cell lane, following the manufacturer's protocol. Image analysis, base calling, and quality scoring of the run were processed using the manufacturer's software Real Time Analysis (RTA 1.13.48) and followed by generation of FASTQ sequence files by CASAVA.

2.5. RNA-seq data processing and analysis

Mouse RNA-seq reads were mapped against the *Mus musculus* reference genome (GRCm38) with STAR/2.5.3a (Dobin et al., 2013) using ENCODE parameters. Genes and isoforms were quantified with RSEM/2.3.0 (Li and Dewey, 2011) with default parameters using the gencode.M15 annotation. Likewise, rat RNA-seq reads were mapped against the *Rattus norvegicus* reference genome (Rnor6.0) whereas the Rnor6.0.92 annotation was used for gene and isoform quantification. The original raw and processed data are available from the Gene Expression Omnibus, accession number GSE226517 (https://www.ncbi.nlm.nih.gov/geo/query/acc.cgi?acc=GSE226517).

Differential expression analysis was performed with the R package DESeq2/1.18 (Love et al., 2014). The regularized log transformation of the counts was used for plotting. Genes with FDR $< 5\%$ and $|FC| > 1.5$ were considered significantly differentially expressed. Heatmaps were drawn with the R package 'ggplot2' using Z-score normalisation and the PCA was done with the 'prcomp' R function. Gene Ontology (GO) enrichment analyses (Ashburner et al., 2000; Gene Ontology Consortium, 2021) were performed on the lists of genes upregulated or downregulated to identify the biological processes (BP) and cellular components (CC) modified by the treatments. Similarly, the Kyoto Encyclopaedia of Genes and Genomes (KEGG) database (Kanehisa and Goto, 2000) was used to identify molecular pathways modified after treatment. GO and KEGG analyses were performed with Enrichr (Chen et al., 2013; Kuleshov et al., 2016; Xie et al., 2021). In addition, Gene Set Enrichment Analyses (GSEA) (Subramanian et al., 2005; Mootha et al., 2003) were performed with the mouse and the rat expression datasets to evaluate whether the gene expression changes induced by the treatment matched any well-known biological process as defined by the Hallmark Gene Sets.

2.6. Real-time quantitative reverse transcription polymerase chain reaction (qRT-PCR)

The High-Capacity cDNA Reverse Transcription Kit (Applied Biosystems, Madrid, Spain) was used to reverse transcribe equal quantities of total RNA. Then, an equal amount (15 ng) of cDNA was used per sample for qRT-PCR analysis, for which we used the SensiFAST Probe Hi-ROX kit (Bioline, Barcelona, Spain). Assays were run in duplicate with the following TaqMan probes (Life Technologies, Madrid, Spain): Mm99999915_g1 (Gapdh, glyceraldehyde 3-phosphate dehydrogenase; used as the internal control gene), Mm00499876_m1 (Slc17a6, solute carrier family 17 [sodium-dependent inorganic phosphate cotransporter], member 6 - vesicular glutamate transporter 2), Mm00436615_m1 (Slc2a4, solute carrier family 2 [facilitated glucose transporter], member 4 - Glut4), Mm00460641_m1 (Camk1g, calcium/calmodulin-dependent protein kinase I gamma), Mm00446296_m1 (Ngfr, nerve growth factor receptor [TNFR superfamily, member 16]), Mm01226041_m1 (Kcnq5, potassium voltage-gated channel, subfamily Q, member 5), Mm00517529_m1 (Chrna6, cholinergic receptor, nicotinic, alpha polypeptide 6), Mm00479438_m1 (Nptx2, neuronal pentraxin 2), Mm00465816_m1 (Etv5, ets variant 5), and Mm00436767_m1 (Spp1, secreted phosphoprotein 1 - osteopontin), Mm04230607_s1 (Bdnf, brain-derived neurotrophic factor). Reaction mixtures (10 μl) were incubated at 50 °C for 2 min, followed by incubation at 95 °C for 10 min, and then by 40 cycles of PCR, each at 95 °C for 15 s and 60 °C for 1 min. A 7900 HT Real-Time PCR System (Applied Biosystems) was used for real-time fluorescence detection, and the Expression Suite software was used to analyse the threshold cycles (Ct). The relative quantification method (ΔΔCt) was used to calculate the target gene expression for group comparisons.

2.7. Immunohistochemical labelling

Rat vestibular ganglion sections were immunolabelled with antibodies against two proteins of interest, fibroblast growth factor 12 (encoded by the *Fgf12* gene; rabbit polyclonal, Proteintech 13,784–1-AP, RRID: AB_2103928, 1/500), and osteopontin/SPP1 (encoded by the *Spp1* gene; goat polyclonal, R&D Systems AF808, RRID: AB_2194992, 1/200). An antibody against the neurofilament heavy polypeptide (NFH; mouse monoclonal IgG1, Sigma-Aldrich, clone N52, Chemicon MAB5266, RRID: AB_2149763, 1/1000) was used to counterstain the ganglion. Additional information on these antibodies is provided in Suppl. Table S2. The following Alexa-fluor-conjugated donkey secondary antibodies from Invitrogen were used at 1/500: 488-anti-mouse IgG (cat. # A21202), 555-anti-rabbit IgG (cat. # A31572) and 647-anti-goat IgG (cat. # A21447). Briefly, free-floating sections were incubated for simultaneous permeation and blocking in PBS with 0.5% Triton-X-100 and 20% donkey serum for 90 min at room temperature (RT). Then, they were sequentially incubated with the primary and the secondary antibodies, in both cases in 0.1% Triton-X-100 and 1% donkey serum for 24 h at 4 °C with gentle rocking. The sections were thoroughly rinsed in PBS after each incubation, and finally mounted in Mowiol medium.

2.8. RNAscope in situ hybridization

Rat vestibular ganglion sections were processed for RNAscope and immunofluorescence following the protocol described by Reijntjes et al. (2021). As demonstrated for the auditory ganglion, this approach is

useful for the quantitative analysis of RNA expression (Kersigo et al., 2018). We used the RNAscope Multiplex Fluorescent Reagent Kit v2 (cat. # 323100, ACD Bio-Techne) with the following probes: Rn-Etv5-*Rattus norvegicus* ets variant 5 (Etv5) mRNA (cat. # 427061) and Rn-Ppib-C3 - *Rattus norvegicus* peptidylprolyl isomerase B (Ppib) mRNA (cat. # 313921-C3) as positive control. To label the probes, we used the fluorophores Opal 520 (cat. # FP1487001KT, Akoya Biosciences) and Opal 570 (cat. # FP1488001KT). Briefly, free-floating ganglion sections were washed in RNAscope Wash Buffer, dehydrated with graded concentrations of methanol, then rehydrated and washed at RT. Next, tissues were treated with Protease III solution for 8 min at RT and washed. The sections were then placed in slides and exposed to a mixture of the Etv5-C1 and Ppib-C3 probes (50:1, as indicated by the manufacturer) for 15 h at 40 °C using the HybEZ™ II Oven (cat. # 321720, ACD). Afterwards, tissues were washed and incubated in amplification solutions Amp1, Amp2 and Amp3 for 35, 20, and 35 min, respectively, at 40 °C. For signal detection, HRP-C1 and HRP-C3 solutions were added to the sections for 15 min each at 40 °C, followed by a 30 min incubation of TSA-diluted Opal 520 and Opal 570 at 40 °C. After washing, the sections were processed for NF-H immunostaining with the N52 antibody and mounted following the protocol described above.

2.9. Image acquisition and analysis

Tissue sections were observed in a Zeiss LSM 880 confocal microscope. Acquisition settings were maintained across sections from the different treatment groups. The ImageJ software (National Institute of Mental Health, Bethesda, Maryland, US) was used for image quantification. To measure immunochemical labelling, images were obtained with a 63× objective (1.4 NA, oil) as Z-stacks of 50 planes taken at 0.4 µm intervals. Then, maximum intensity projections were obtained from 6 consecutive planes spanning a total of 2.4 µm. The fluorescence intensity was then measured using a region of interest of 100 μm^2 and averaged for 30–40 cells per sample. For RNAscope analysis, 3 different areas were imaged from each sample with a 40× objective (1.3 NA, oil). The corresponding Z-stacks were made of 12 planes taken at 0.5 µm intervals. The maximum intensity projection of each picture was obtained and then the number of Etv5 and Ppib mRNA puncta were counted automatically by employing the Find Maxima tool. The number of neurons was counted manually in the same image to calculate the number of puncta per neuron. Results were averaged across pictures of the same sample. Analysis settings were maintained in all pictures and conditions.

2.10. Statistics

Data are shown as X ± SE. For group comparisons, we used the Student's *t*-test or ANOVA analysis followed by Duncan's test, as appropriate. The significance level was set at 0.05.

3. Results

3.1. Subchronic vestibular toxicity modifies gene expression in the vestibular ganglion of rats and mice

In previous studies, we described that male 129S1 mice treated with 30 mM of IDPN in the drinking water for 8 weeks (Greguske et al., 2019) and male Long-Evans rats treated with 20 mM of IDPN for 4 weeks (Sedó-Cabezón et al., 2015) show similar losses in vestibular function and equivalent capacity for recovery. In both species, these function loss and recovery associate with HC detachment and synaptic uncoupling followed by reattachment and synaptic repair in the vestibular epithelium. In the present study, mice and rats exposed to these respective concentrations of IDPN showed the expected progressive decline in vestibular function (data not shown) and were euthanized at the corresponding time points to study RNA expression in the vestibular ganglion.

In the mouse RNA-seq study, a principal component analysis (PCA) with the 500 most variable genes differentiated between control ($n = 3$) and treated (n = 3) animals according to PC1 (49.8% of variance) and PC2 (29.1% of variance) (Fig. 1A). We found 956 differentially expressed genes (DEG), of which 436 were upregulated and 520 were downregulated. Looking at the 50 most significantly altered genes revealed that the majority (48/50) of these top genes were downregulated in mice treated with IDPN compared to control mice (Fig. 1B). Displaying all the genes in a volcano plot according to $\log_2$-Fold_Change and log-Padj also revealed that more downregulated genes than upregulated genes showed higher differences between groups and higher significance (Fig. 1C).

In rats, PCA analysis of the 500 most variable genes generated a PC1 that gathered 59.4% of the variance and separated control (n = 3) and IDPN (n = 3) rats (Fig. 2A). These groups of animals showed 919 DEGs, where 368 were upregulated and 551 were downregulated. Among the 50 most significantly altered genes, 43 were downregulated and 7 were upregulated (Fig. 2B). As performed in mice, the volcano representation of the rat data revealed a stronger downregulation response than upregulation response because of the subchronic ototoxicity (Fig. 2C).

3.2. Subchronic vestibular toxicity downregulates the expression of genes encoding for proteins involved in synaptic function, neuronal excitability, and neurite maturation

We hypothesized that the most important gene expression responses to subchronic vestibular toxicity would be conserved across species. Therefore, we compared the lists of DEGs in mice and rats exposed to subchronic IDPN and identified 213 genes whose expression was significantly modified in both species. Although 4 of these genes showed different responses (that is, they were upregulated in one species and downregulated in the other), the other 209 were regulated similarly in both species (Suppl. Table S3). These common genes are highlighted in the volcano plots of the mouse (Fig. 1C) and rat (Fig. 2C). These plots highlight the fact that many of these genes were among those showing the greatest significance and the largest change in expression in both species.

Gene Ontology (GO) enrichment analyses were performed to identify biological processes (BP) and cell components (CC) associated with the up- or downregulated genes in each species and with the genes similarly regulated in both species. The analysis of the list of downregulated genes in the mouse resulted in 27 BP and 38 CC terms with significant (Padj<0.05) alterations in expression. These included many terms related to synaptic structure and function, such as “synapse organization”, “clathrin-dependent endocytosis”, “synaptic vesicle membrane”, or “clathrin coat of coated pit”. In the rat, the number of significant terms was lower, 11 BP and 8 CC, but these included terms also related to synapses, including “synapse organization”, “synaptic transmission, glutamatergic”, “synaptic vesicle membrane”, and “clathrin coat”. The robustness of the downregulation of genes encoding for synaptic machinery proteins was confirmed by the GO analysis of the genes similarly regulated in both species. This analysis yielded 20 BPs and 9 CC with Padj<0.05. As shown in Fig. 3, significant downregulation was found in the synaptic BP (Fig. 3A) and CC (Fig. 3B) terms. In addition, other terms identified by the enrichment analysis were also related to synaptic function. Thus, the effect found in terms related to inositol phosphate metabolism was associated with the effect on the phosphatase genes *Synj1*, *Synj2* and *Inpp5j*, which have prominent roles in synapses. Similarly, the Kyoto Encyclopedia of Genes and Genomes (KEEG) pathway analysis identified the “inositol phosphate metabolism”, the “synaptic vesicle cycle” and the “phosphatidylinositol signalling system” terms as significant after the adjustment for multiple comparisons (Fig. 3C). Taken together, the RNA-seq data revealed a robust downregulation of the expression of genes involved in synaptic neurotransmission. Downregulated genes included many genes encoding for presynaptic proteins

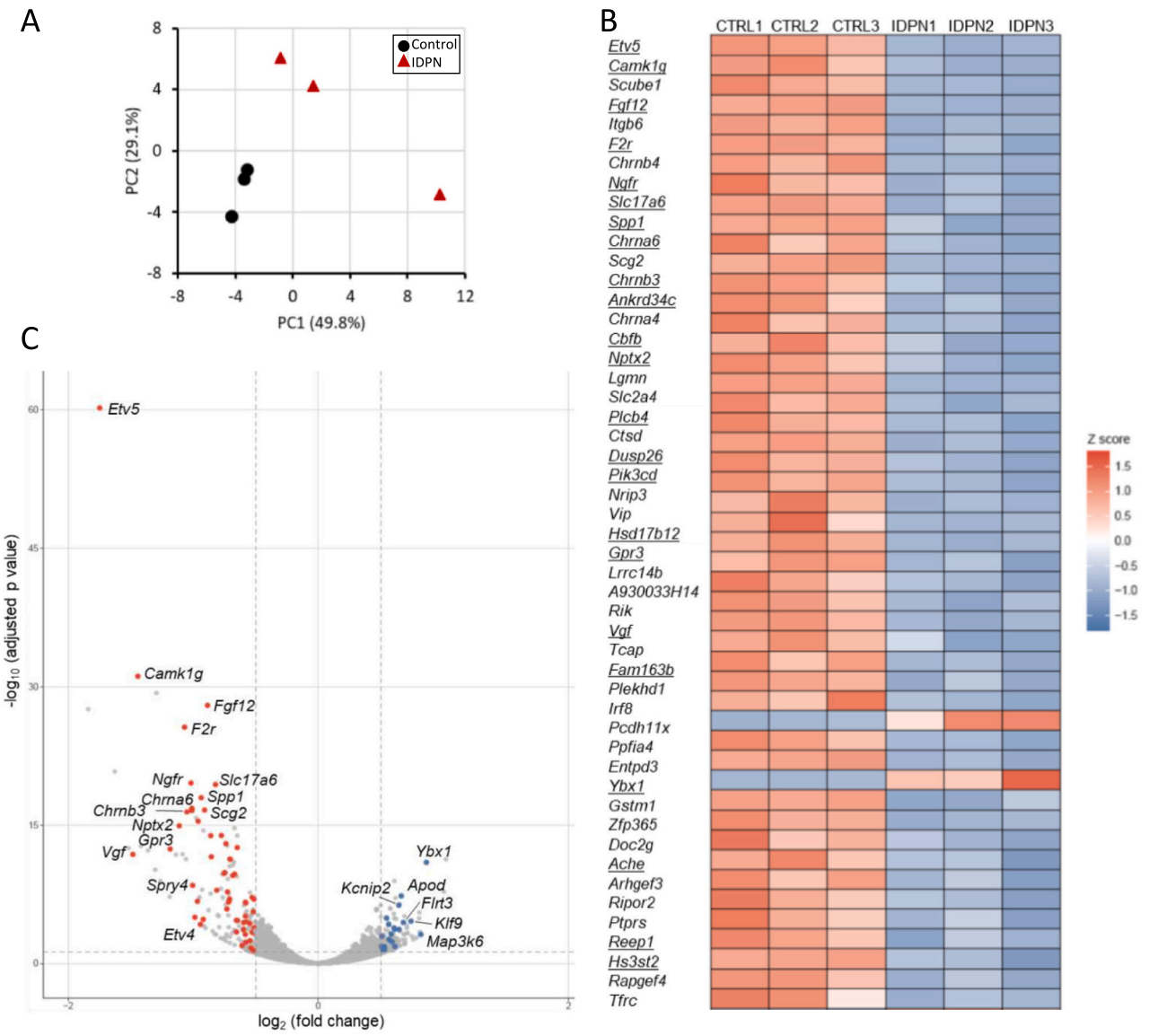

Fig. 1. RNA-seq analysis of the effect of subchronic 3,3′-iminodipropionitrile (IDPN) exposure on gene expression in the vestibular ganglion of the mouse. Treated mice were exposed to 30 mM of IDPN in the drinking water for 8 weeks. **A.** Principal Component Analysis (PCA) with the 500 most variable genes grouped animals according treatment group in PC1 and PC2, which gathered 79% of the variance. **B.** Heatmap of the 50 top differentially expressed genes (DEG), ordered by level of statistical significance after adjustment for multiple comparisons. Underlined genes are those that were also found to have a similar modification in expression in the rat experiment. **C.** Volcano plot of all genes according to statistical significance and fold change in expression. Coloured dots correspond to genes whose expression was found also significantly reduced (red) or increased (blue) in rats. Selected genes are identified with their name. (For interpretation of the references to colour in this figure legend, the reader is referred to the web version of this article.)

required for synaptic vesicle function and glutamate exocytosis (*Unc13a*, *Slc17a6*, *Synj1*, *Vamp2*, *Ap2b1*, *Syngr1*, *Syngr3*, *Sv2a*, *Eps15*, *Atp6v1a*, *Napb*, *Slc38a1*, and others), but also genes of postsynaptic proteins of both glutamatergic (*Gria2*, *Kcnq5*) and cholinergic (*Chrna6*, *Chrna3*, *Ache*) synapses.

As noted in the heat maps and volcano plots (Figs. 1 and 2), the upregulated response was weaker than the downregulated response. Enrichment analysis on the list of genes up-regulated in both species provided a list of 19 BP terms (Padj <0.05), with "myelination", and "negative regulation of cellular macromolecule biosynthetic process" at the top (Fig. 3D). Upregulated genes related to myelination included *Apod*, *Klf9*, *Mpz*, *Sox10*, *Bcas1*, *Atrn*, and *Mbp*. In the other analyses, the list of commonly upregulated genes yielded one single CC that retained statistical significance after correction ("Sin3 complex") and no significant KEEG pathway. The greater robustness of the downregulated response in comparison to the upregulated response was also revealed by the fact that the analysis of the complete list of DEGs, including both up and downregulated genes, highlighted synaptic components above all. Thus, the first seven BP terms identified on this list were "synapse organization", "synaptic transmission, glutamatergic", "synaptic transmission, cholinergic", "regulation of signal transduction", "chemical synaptic transmission", "glycerophospholipid biosynthetic process", and "neurotransmitter transport".

The mouse and the rat expression datasets also underwent GSEA as an alternate approach to reveal patterns of gene expression modification. In contrast to the previous analyses, GSEA with the Hallmark Gene Sets did not identify any robust downregulated responses. Thus, no gene sets were significantly (FDR/q-val < 0.05) enriched in Control versus IDPN mice, and only one ("oxidative phosphorylation") in Control versus IDPN rats. Conversely, 9 and 6 gene sets were found to be enriched in IDPN mice and rats compared to their controls, respectively, and 3 of these were enriched in both species: "TNFA signalling via

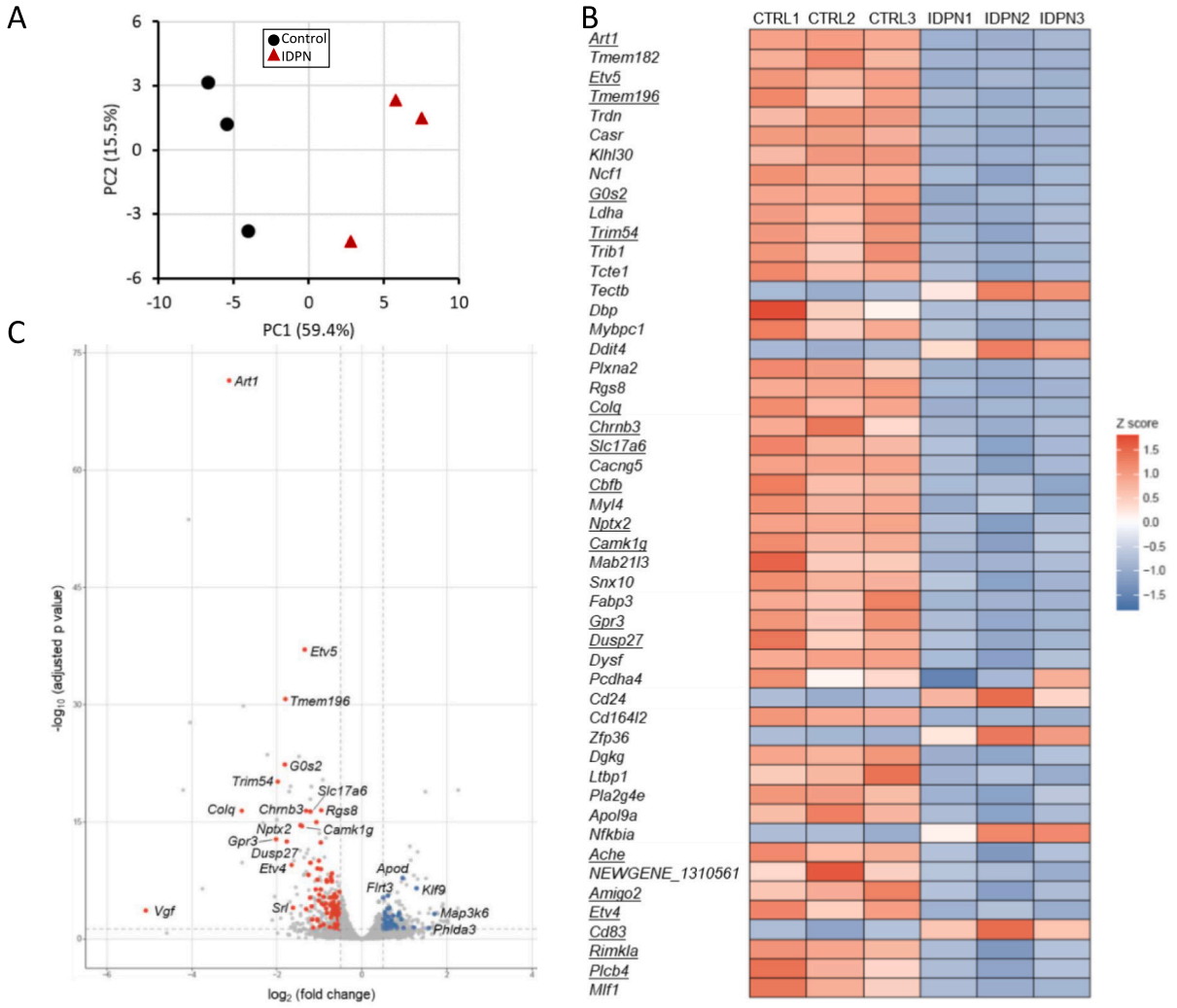

Fig. 2. RNA-seq analysis of the effect of subchronic 3,3′-iminodipropionitrile (IDPN) exposure on gene expression in the vestibular ganglion of the rat. Treated rats were exposed to 20 mM of IDPN in the drinking water for 4 weeks. **A.** Principal Component Analysis (PCA) with the 500 most variable genes grouped animals according treatment group in PC1, which explained 59% of the variance. **B.** Heatmap of the 50 top differentially expressed genes (DEG), ordered by level of statistical significance after adjustment for multiple comparisons. Underlined genes are those that were also found to have a similar modification in expression in the mouse experiment. **C.** Volcano plot of all genes according to statistical significance and fold change in expression. Coloured dots correspond to genes whose expression was found also significantly reduced (red) or increased (blue) in mice. Selected genes are identified with their name. (For interpretation of the references to colour in this figure legend, the reader is referred to the web version of this article.)

NFKB", "G2M checkpoint", and "apoptosis". However, these gene sets did not relate to the most robust expression responses shared by mice and rats exposed to subchronic IDPN. As such, comparing the list of 209 common DEGs in mice and rats with the genes of these three upregulated sets resulted in virtually no overlap: only two genes (*Klf9*, *Rhob*) were coincident with the "TNFA signalling via NFKB" set, none with the "G2M checkpoint", and two (*Rhob*, *Pdcd4*) with the "apoptosis" set.

To complete the transcriptomic data analysis, we manually evaluated the list of the top DEGs common in mice and rats; we organized them by a composite rank by adding the ranks of each species according to their Padj value (Suppl. Table S3). In addition to the responses identified by the GO and pathway analyses previously discussed, we observed other expression changes of interest. We noticed a robust decrease in the expression of genes that have been associated with neuronal activity: *Camk1g* (rank = 2), *Slc17a6* (rank = 3), and *Nptx2* (rank = 6). The data also showed a strong down regulation of several transcription factors and receptors, including *Etv5* (rank = 1), *Gpr3* (rank = 7), *Etv4* (rank = 24), *Ngfr* (rank = 21), and *Vgf* (rank = 33), as well as decreased expression of *Fgf12* (rank = 8), a positive regulator of voltage-gated sodium channels. As will be detailed in the Discussion section, these data suggested that the loss of BDNF input from the epithelium could be responsible, at least in part, for the observed expression changes in the ganglion. As BDNF, together with NT3, has critical roles in auditory and vestibular ganglion neuron development and survival by signalling through the neurotrophic tyrosine kinase receptors type 2 and 3 (Fritzsch et al., 1998; Fariñas et al., 2001; Fritzsch et al., 2016), we looked in our RNA-seq results for expression of the corresponding genes, *Ntrk2* and *Ntrk3*. The data demonstrated expression of both receptor genes in the ganglion, but no change in this expression after IDPN. Mean, log2 fold change and Padj values were as follows: mouse *Ntrk2*, 9446, −0.117, 0.523; mouse *Ntrk3*, 4517, 0.089, 0.759; rat *Ntrk2*, 11,315, −0.032, 0.929; rat *Ntrk3*, 2113, −0.226, 0.248.

3.3. *Changes in mRNA expression were confirmed by qRT-PCR, RNAscope in-situ hybridisation, and immunohistochemistry*

To corroborate the changes in gene expression revealed by the RNA-seq data, we sought to replicate the results using qRT-PCR. To this end, we used a new set of control and sub-chronic IDPN mice ($n = 9$/group) and compared the expression of six genes that were selected among the

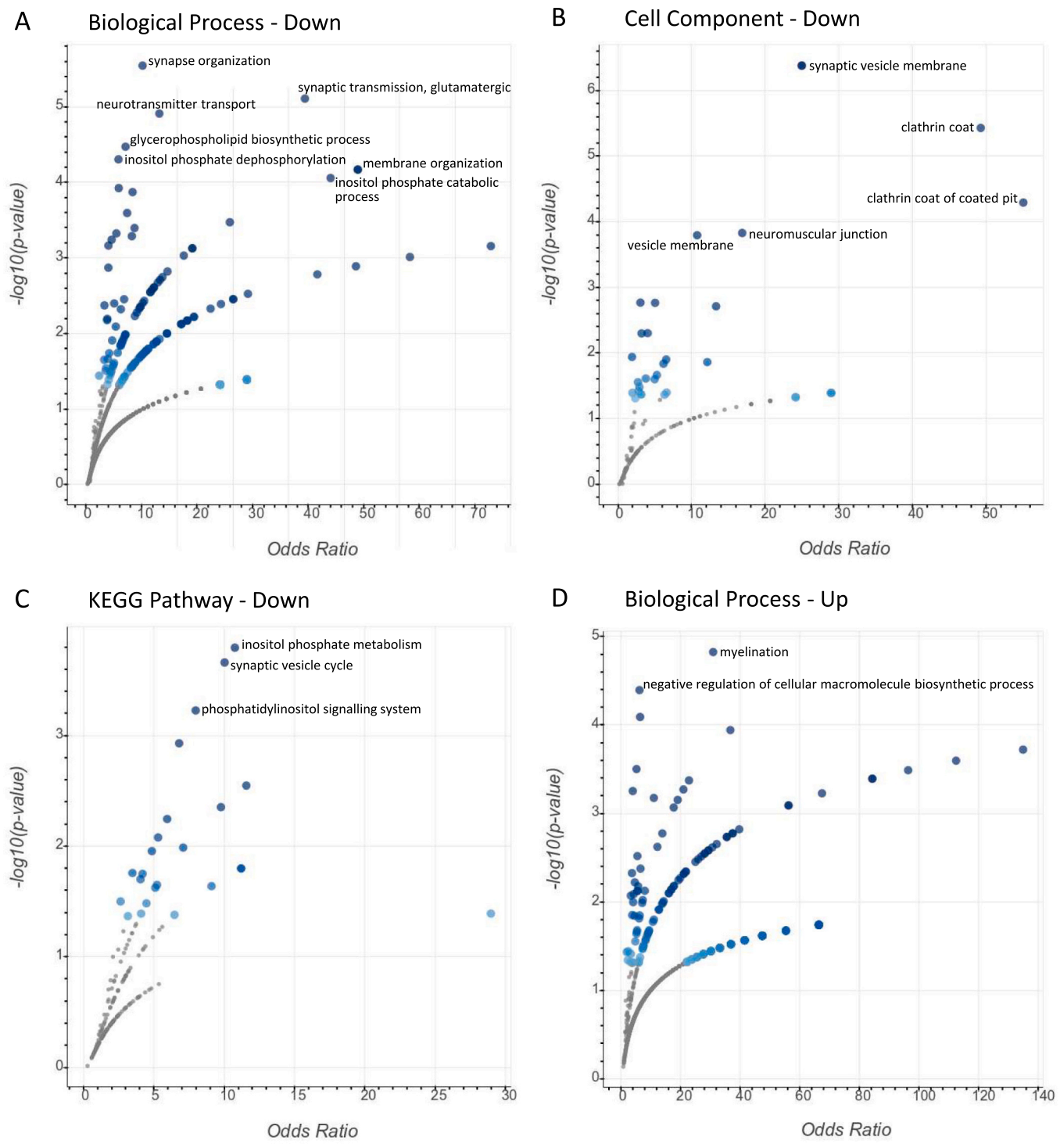

Fig. 3. Enrichment analyses of the genes differentially expressed (DEG) in both rats and mice after subchronic 3,3′-iminodipropionitrile (IDPN) exposure. **A-C:** Biological processes (**A**), cell components (**B**) and Kyoto Encyclopaedia of Genes and Genomes pathways (**C**) analyses of the downregulated genes. **D:** Biological process analysis of the up-regulated genes.

top 20 as ranked by their Padj value in this species. These were *Camk1g* (rank = 2; log2FC = −1.614; Padj = 5.74E-32), *Slc17a6* (8; −0.866; 1.46E-20), *Ngfr* (9; −1.107; 1.46E-20), *Chrna6* (11; −1.114; 1.06E-17), *Nptx2* (18; −1.279; 1.25E-15), and *Slc2a4* (19; −1.009; 3.79E-15). We included two additional DEGs for which we had probes from previous research, *Kcnq5* (72; −0.798; 1.45E-7), and *Homer1* (384; +0.833; 0.006). As shown in Fig. 4A, the qRT-PCR data matched the RNA-seq data for all genes. Thus, these genes showed significantly increased (*Homer1*) or decreased (*Camk1g*, *Slc17a6*, *Ngfr*, *Chrna6*, *Nptx2*, *Slc2a4*, *Kcnq5*) expression in agreement with the result of the RNA-seq analysis. Results of the Students *t*-test were as follows: *Camk1g*, $t(12) = 7.51$, $p < 0.001$; *Slc17a6*, $t(11) = 9.66$, $p < 0.001$; *Ngfr*, $t(12) = 4.00$, $p = 0.002$; *Chrna6*, $t(16) = 3.54$, $p = 0.003$; *Nptx2*, $t(16) = 6.41$, $p < 0.001$; *Slc2a4*, $t(13) = 6.36$, $p < 0.001$; *Kcnq5*, $t(16) = 3.21$, $p = 0.006$; *Homer1*, $t(13) = 2.28$, $p = 0.040$. Using the same control and sub-chronic IDPN mice, we also assessed the expression of *Bdnf* in the sensory epithelium. Fig. 4B

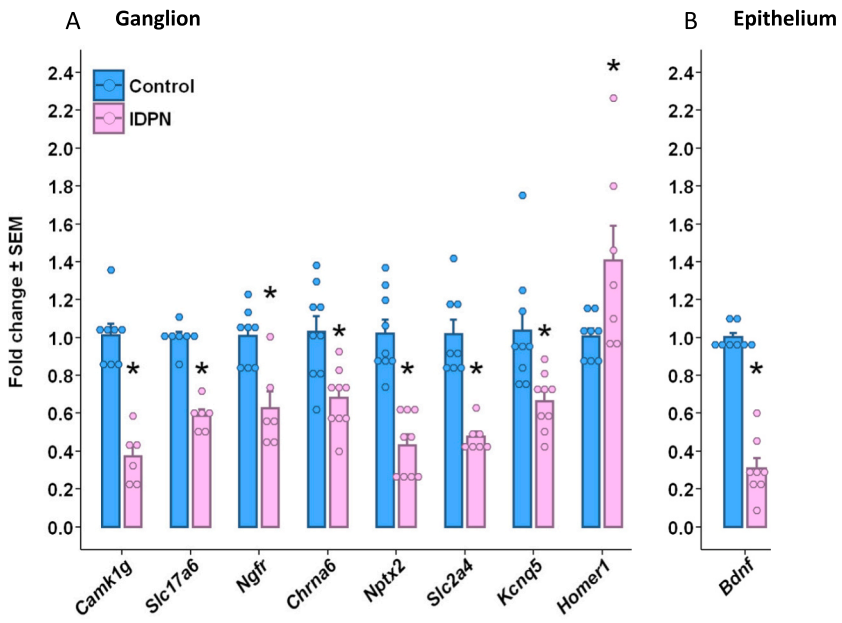

Fig. 4. Effect of subchronic 3,3′-iminodipropionitrile (IDPN) exposure on gene expression in the vestibular ganglion and epithelium of the mouse analysed by qRT-PCR. Treated mice were exposed to 30 mM of IDPN in the drinking water for 8 weeks. Bars show X ± SE (n = 6–9 animals/group), expressed as fold change from control mean. *: $p < 0.05$, Student's t-test.

shows that *Bdnf* expression was strongly down regulated in the epithelium after sub-chronic IDPN (t(14) = 11.48, p < 0.001).

We also used RNA-scope *in situ* hybridisation analysis to evaluate the expression response of the top gene *Etv5* (3; −1345; 9.2E-38) triggered in the vestibular ganglion of the rat by sub-chronic ototoxicity. This analysis was performed on archival ganglia from 4 control and 4 IDPN rats from experiments reported elsewhere (Sedó-Cabezón et al., 2015). As shown in Fig. 5, *Etv5* was expressed by both types of vestibular ganglion neurons, those that express high levels of NFH protein and those that do not. After subchronic IDPN, no change was recorded in the number of RNA-scope puncta that revealed mRNA expression of the control gene *Ppib* (t(6) = 0.989, p = 0.361), whereas a significant decrease was recorded for *Etv5* mRNA expression (t(6) = 2.772, p = 0.032). There was no change in the number of neurons (t(6) = 0.495, p = 0.638), so a similar significant decrease in *Etv5* expression was found (t(6) = 2.63, p = 0.039) if the number of puncta per neuron was considered instead of the total number of puncta.

For two genes, *Fgf12* (55; −0.704; 4.11E-09) and *Spp1* (gene product also known as oncomodulin - 277; −0.410; 0.00128) (antibodies available in Suppl. Table S2), we sought to evaluate whether the changes in mRNA levels resulted in protein expression changes. To this end, we again used archival ganglia from control and IDPN rats. As shown in Fig. 6, these antibodies labelled both large and small vestibular ganglion neurons, and IDPN caused a significant reduction in the label: the fluorescence intensity of the Spp1 immunolabelling was smaller in the IDPN rats than in the control rats (t(6) = 4.28, p = 0.005), as was the intensity of the Fgf12 immunolabelling (t(6) = 2.69, p = 0.036).

3.4. Changes in mRNA expression in the vestibular ganglion neurons associate with HC damage or loss in the vestibular epithelium

Two final experiments were performed to establish the association of the changes in mRNA expression in the vestibular ganglion to ototoxicity-induced events in the vestibular epithelium. First, we evaluated whether a recovery in gene expression would occur if animals were allowed to survive after the end of the treatment. We used mouse archival samples from control ganglia, ganglia of mice treated subchronically with IDPN, and mice given a 12-week washout period after the end of the 8-week treatment, in which reattachment between HCs and afferent terminals has been demonstrated to occur (Greguske et al., 2019). As shown in Fig. 7, variable degrees of recovery occurred, from null (*Slc17a6*) to full (*Spp1*), but no gene showed a higher change in expression after washout than after the treatment. Statistical results in this experiment were as follows: *Etv5*, F (2, 21) = 28.29, $p < 0.001$; *Camk1g*, F (2, 21) = 8.15, $p = 0.002$; *Slc17a6*, F (2,15) = 6.24, $p = 0.011$; *Nptx2*, F (2, 15) = 2.98, $p = 0.082$; *Spp1*, F (2, 21) = 8.35, $p = 0.002$.

Finally, we evaluated whether an ototoxic lesion protocol that causes irreversible loss of HCs (Saldaña-Ruíz et al., 2013) would cause a similar down-regulation response, comparable to the reversible lesion caused by sub-chronic IDPN. We compared expression in control mice and in mice where the lesion was confirmed by a large, significant (p < 0.001) reduction in the nose-neck-tail angle in the tail-lift reflex, which reflects a loss of vestibular function. The qRT-PCR data, presented in Fig. 8, demonstrated that the loss of HCs resulted in a significant drop in expression of *Etv5*, *Camk1g*, *Slc17a6*, *Nptx2*, and *Spp1*, indicating a comparable downregulation response. Results of the Students t-test were: *Etv5*, t(16) = 10.80, p < 0.001; *Camk1g*, t(16) = 16.42, p < 0.001; Slc17a6, t(12) = 3.53, $p = 0.004$; *Nptx2*, t(12) = 4.68, $p = 0.001$; *Spp1*, t (16) = 13.27, $p < 0.001$.

4. Discussion

After ototoxicant-induced HC loss, vestibular ganglion neurons undergo a slow process of degeneration (Wang et al., 2017), even if the afferent terminals and neuronal cell bodies initially showed essential resiliency (Llorens and Demêmes, 1994; Wang et al., 2017). This can be explained by the selectivity of the ototoxic action on the HCs (Llorens and Demêmes, 1994; O'Sullivan et al., 2017; Kenyon et al., 2021; Steyger, 2021) and the dependency of the neurons on the trophic support given by the HC, which is mostly based on BDNF signalling (Fritzsch et al., 2004; Elliott et al., 2021). Additionally, increasing evidence indicates that pathologies of the afferent terminals, the HC-afferent synapses, and the adhesion complexes between HCs and afferents, followed by phenomena of little, partial or full repair, are important outcomes of sub-maximal or chronic ototoxic exposure models in which intact or damaged HCs survive (Sedó-Cabezón et al., 2015; Gaboyard-Niay et al., 2016; Sultemeier and Hoffman, 2017; Greguske et al., 2019; Cassel et al., 2019; Kim et al., 2022; Maroto et al., 2022). The present study

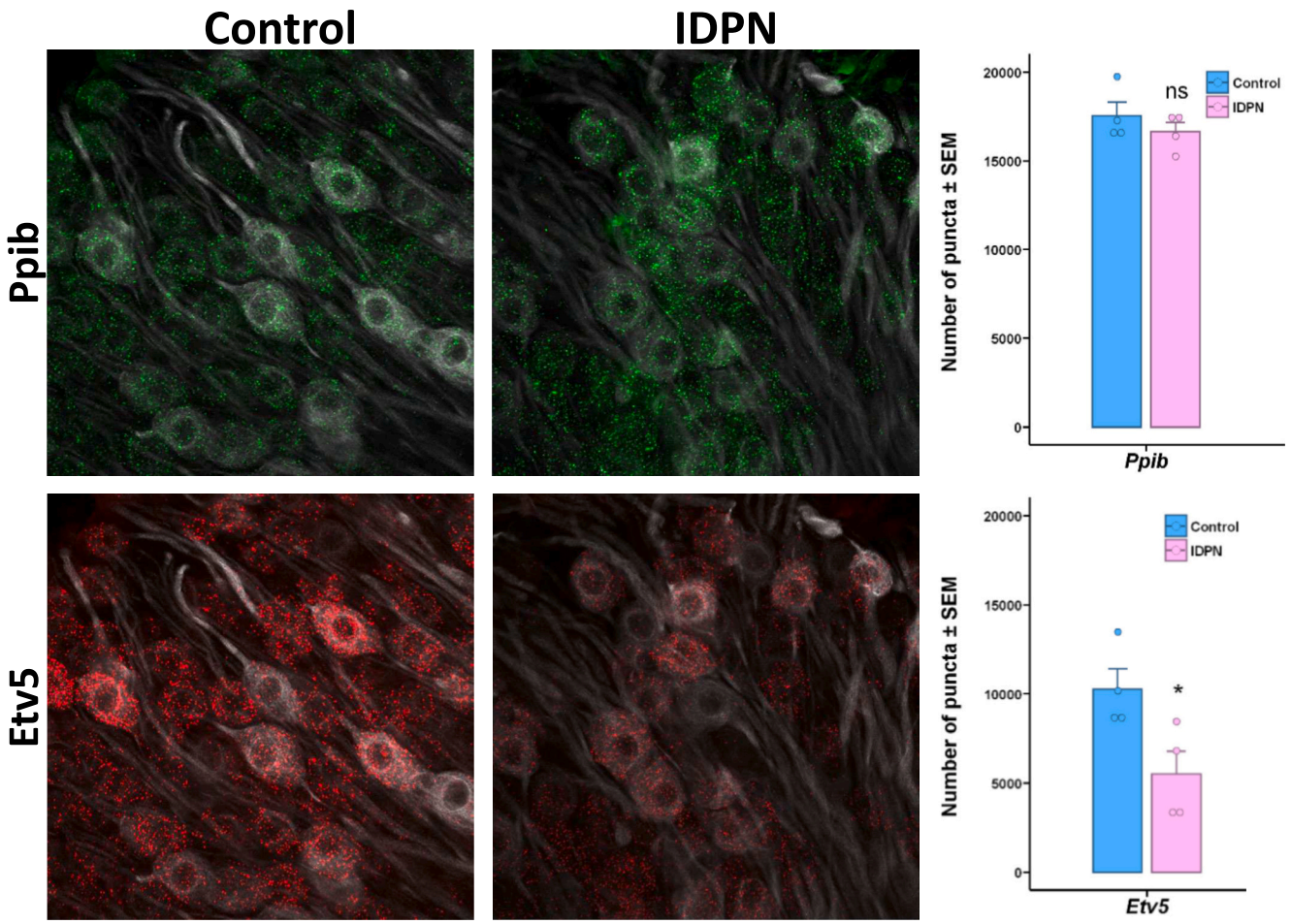

Fig. 5. Effect of subchronic 3,3′-iminodipropionitrile (IDPN) exposure on gene expression in the vestibular ganglion analysed by *in situ* hybridisation RNA-scope. Treated rats were exposed to 20 mM of IDPN in the drinking water for 4 weeks. **Left:** Representative RNA-scope images are shown separately for the control gene Ppib (green, upper panels) and the Etv5 gene (red, lower panels), which was found significantly downregulated by RNA-seq. Ganglion sections were counterstained by NFH immunohistochemistry (grey). Note that RNA-scope signals were found in both NFH-rich and NFH-poor neurons. Images are maximum projections of 12 consecutive planes spanning 6 μm. Scale bar: 20 μm. **Right:** Bars show the number of puncta (X ± SE) from control and treated rats ($n = 4$/group). *: significantly different ($p < 0.05$) from control mean, Student's t-test. (For interpretation of the references to colour in this figure legend, the reader is referred to the web version of this article.)

examined the gene expression response of the vestibular ganglion associated with the HC-afferent detachment caused by subchronic IDPN exposure and identified several responses, including a robust down-regulation of genes encoding proteins involved in synaptic function.

The cellular pathology caused by IDPN in the vestibular epithelium has been well characterized. This low molecular weight nitrile and other similar compounds (allylnitrile, *cis*-crotononitrile) have a selective damaging effect on the sensory HCs of the inner ear (Llorens et al., 1993; Llorens and Demêmes, 1994; Balbuena and Llorens, 2001; Seoane et al., 2001; Balbuena and Llorens, 2003; Boadas-Vaello et al., 2005; Soler-Martín et al., 2007) that makes them a useful tool for HC ablation *in vivo* (Saldaña-Ruíz et al., 2013). In addition, IDPN shows a particularly favourable ratio of vestibular vs systemic toxicity and a remarkable ability of effect accumulation during chronic exposure through drinking water (Llorens et al., 1993; Llorens and Rodríguez-Farré, 1997; Seoane et al., 2001). These favourable features for experimental use allowed the detailed analysis of the damage progression during subchronic exposure, which revealed that the detachment of HCs from their afferent terminals precedes HC loss via extrusion towards the labyrinth lumen (Sedó-Cabezón et al., 2015; Greguske et al., 2019). Recent data indicate that these phenomena may have broad significance, as they have been in part identified in rats exposed to streptomycin, an ototoxic antibiotic with clinical relevance, and in the sensory epithelia from vestibular schwannoma patients (Maroto et al., 2022). Therefore, we selected subchronic IDPN as an adequate model for the initial study of the gene expression response of the vestibular ganglion to subchronic ototoxicity causing reversible deafferentation.

One feature of the IDPN model is its effectiveness in a variety of species, including rats (Llorens et al., 1993; Llorens and Rodríguez-Farré, 1997; Sedó-Cabezón et al., 2015) and mice (Soler-Martín et al., 2007; Greguske et al., 2019). We studied and compared both species as a strategy to identify the expression responses conserved across species, presumably of more importance than species-dependent responses. The concentration of IDPN in the drinking water and the time of exposure were different in rats and mice, but were selected to attain a similar effect in the precise types of animals that we were using. Available data indicates that the final extent and time course of the IDPN effects vary as a function of the species, strain, and sex (Llorens and Rodríguez-Farré, 1997; Boadas-Vaello et al., 2017; Greguske et al., 2019; Greguske et al., 2021), probably due to differences in absorption, metabolism, or excretion of the compound, so different doses and times are needed to reach similar effects for diverse animals. The use of different IDPN concentrations and times of exposure in rats and mice may have been a source of differences in RNA expression between experiments. However, we hypothesized that adjusting the exposure conditions to attain similar levels of vestibular damage would provide more comparable results.

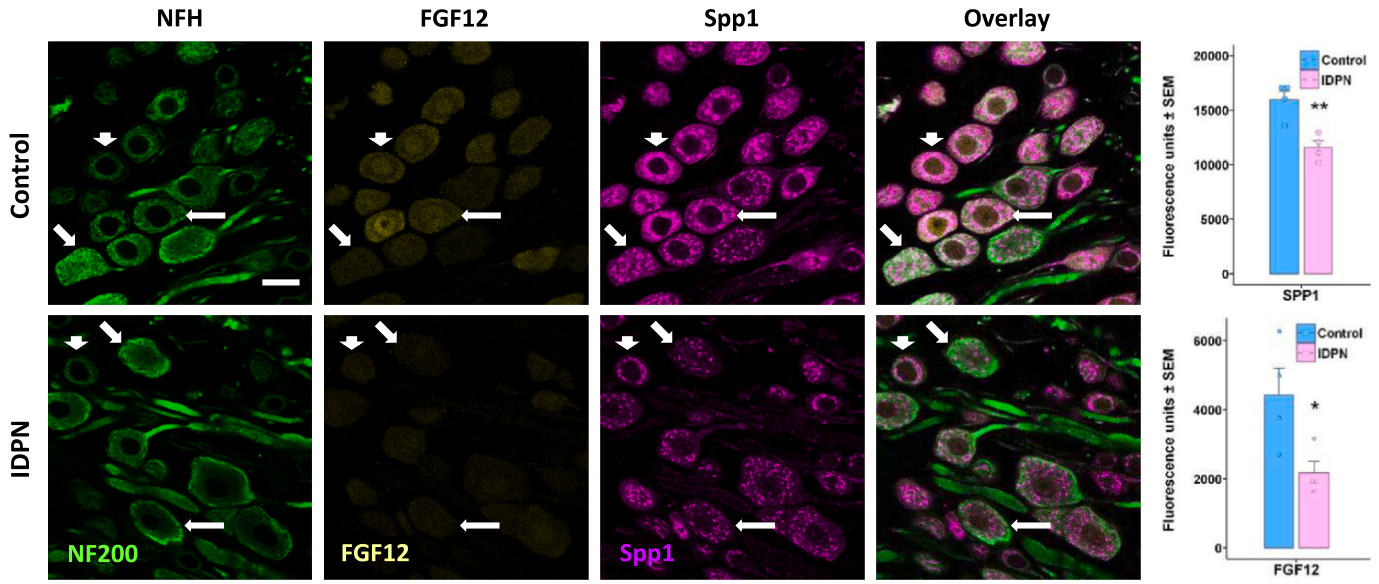

Fig. 6. Effect of subchronic 3,3′-iminodipropionitrile (IDPN) exposure on protein expression in the vestibular ganglion of the rat analysed by immunohistochemistry. Treated rats were exposed to 20 mM of IDPN in the drinking water for 4 weeks. **Left:** Representative images of vestibular ganglion sections immunolabelled with anti-NFH (green), anti-FGF12 (yellow), and anti-Spp1 (violet) antibodies. Images shown are maximum projections of 10 consecutive optical sections spanning 4 μm. Arrows of different length and orientation indicate neurons of similar size and section level in the control and IDPN images for comparison. Scale bar in upper left pannel: 20 μm. **Right:** Bars show fluorescence intensity (arbitrary units, X ± SE) for Spp1 and Fgf12 in control and treated rats (n = 4/group). *, **: significantly different ($p < 0.05$, $p < 0.01$, respectively) from control mean, Student's *t*-test. (For interpretation of the references to colour in this figure legend, the reader is referred to the web version of this article.)

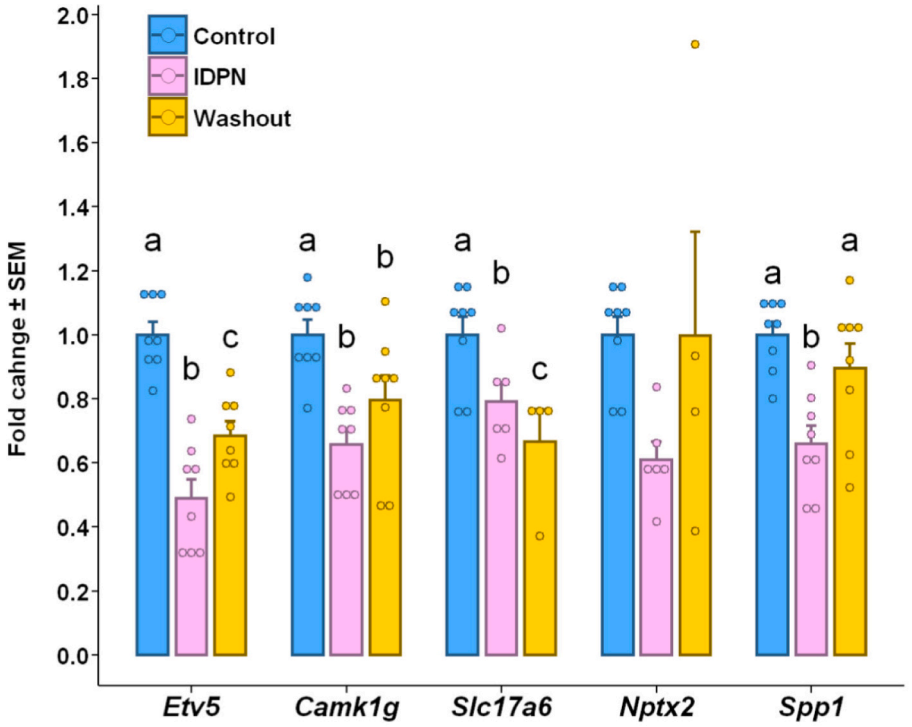

Fig. 7. Effect of subchronic 3,3′-iminodipropionitrile (IDPN) exposure and washout period on gene expression in the vestibular ganglion of the mouse analysed by RT-PCR. Treated mice were exposed to 30 mM of IDPN in the drinking water for 8 weeks and evaluated at the end of exposure or after washout. Data are X ± SE (n = 4–8 animals/group) in fold change respect to control mean. **a, b, c:** Groups not sharing a common letter are different ($p < 0.05$), Duncan's test after significant ANOVA.

Future work may evaluate the role of each factor by, for instance, evaluating the time course of the RNA expression changes in both species.

A limitation of the IDPN model is that this compound is well known to have a direct toxic action on neurons, causing proximal neurofilamentous axonopathy. Animals exposed to this nitrile display an accumulation of neurofilaments in proximal myelinated structures, such as the proximal axon of large neurons (Chou and Hartmann, 1964) and

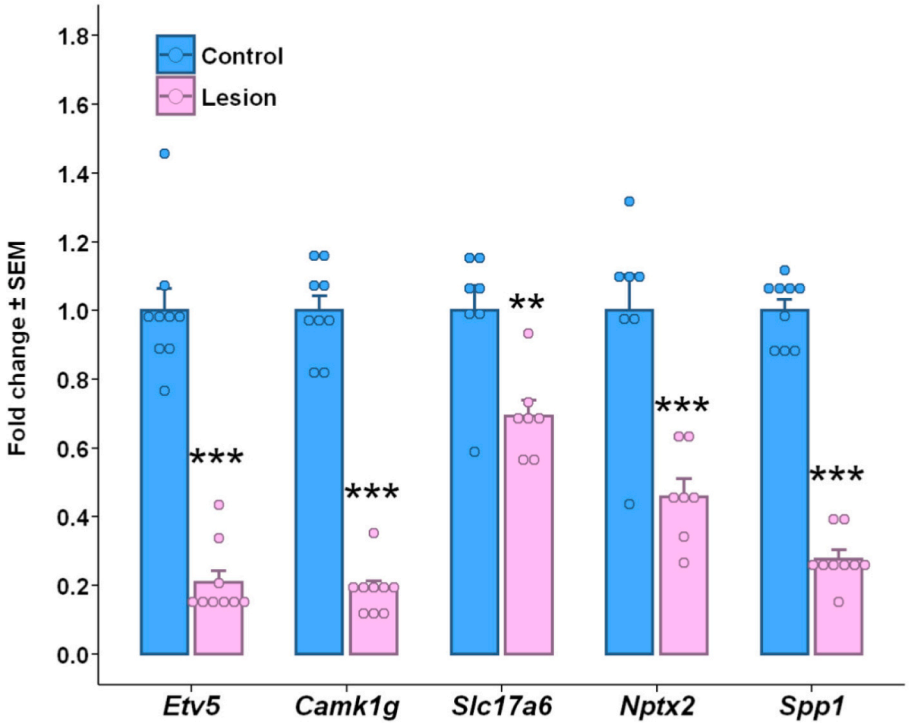

Fig. 8. Effect of HC loss on gene expression in the vestibular ganglion of the mouse analysed by RT-PCR. Lesion mice were co-exposed to 1.2 mmol/kg of allylnitrile and two doses of 100 mg/kg of *trans*-1,2-dichloroethylene to cause HC loss and were examined three weeks after exposure. Data are X ± SE ($n = 7$–9 animals/group) in fold change respect to control mean. **, ***: $p < 0.01$ and $p < 0.001$, respectively, Student's t-test.

the cell body of the vestibular ganglion neurons (Llorens and Demêmes, 1996). This effect associates with a decrease in the axonal transport of neurofilaments (Griffin et al., 1978), but its molecular basis has not been elucidated. Therefore, the gene expression responses identified here could be due to the HC effect or to a direct neuronal effect. However, several of the core gene expression changes recorded in the sub-chronic IDPN rats and mice were also found in the vestibular ganglia of mice suffering deafferentation caused by acute allylnitrile-induced HC loss. In the acute experiment, allylnitrile is ototoxic but does not cause the neurofilamentous axonopathy (Balbuena and Llorens, 2001; Soler-Martín et al., 2011; Saldaña-Ruíz et al., 2013), so the gene expression changes observed were not secondary to an axonopathic action. Therefore, the robust downregulation of *Spp1*, *Etv5*, *Camk1g*, *Slc17a6* and *Nptx2* observed by qRT-PCR in the vestibular ganglion of mice with allylnitrile-induced HC loss supports the conclusion that HC-neuron detachment was the trigger of the downregulation of these and other genes observed by RNA-seq after subchronic IDPN ototoxicity.

In both rats and mice, we observed a more robust down- than up-regulation response after sub-chronic IDPN. Although the vestibular ganglion contains more than one type of cell, the known roles of the differentially expressed genes clearly identified a downregulation of neuronal genes involved in synaptic transmission, and a less robust but significant increase in Schwann cell genes involved in myelinisation. In addition to the gene-sets highlighted by the GO analyses, a robust downregulation of other genes known to be related to neuronal activity was noted (discussed below). By contrast, other effects, as those found by GSEA, appeared less relevant as they differed among species or did not relate to the changes in the expression of the most affected genes. As the IDPN-induced axonopathy has been demonstrated to associate with demyelination and re-myelination (Griffin et al., 1987), the effect on myelin genes can be a direct impact of IDPN on the Schwann cells or, perhaps, a consequence of the action on the vestibular ganglion neurons. Although these effects have been reported at exposure levels higher than those used here, our IDPN exposure model also causes neurofilament alterations (Seoane et al., 2003). In any case, as discussed above, the most robust response was the downregulation of genes that directly responded to the deafferentation and other genes important for synaptic activity. Immunohistochemical analyses of FGF12 and Spp1 supported the conclusion that decreases in gene expression translate into decreases in protein expression.

Interestingly, the downregulated genes encode both pre- and post-synaptic proteins. The observed decrease in GluA2 expression had been described previously in association with the decrease in GluA2-positive synaptic puncta after subchronic exposure, a finding indicative of synaptic uncoupling between the HCs and the afferent terminals (Sedó-Cabezón et al., 2015; Greguske et al., 2019). The present results thus support the notion that this uncoupling may be, at least in part, mediated by postsynaptic gene expression changes. In addition, the present results demonstrate that the ganglion neurons reduce expression of the machinery necessary for glutamate secretion, so a reduction in synaptic transmission must also occur at the synapse between the primary sensory neuron and the second order neuron in the vestibular nuclei. Finally, the downregulation in cholinergic receptor subunits and in acetylcholinesterase suggest that the vestibular ganglion neurons may have changed their response to acetylcholine. Acetylcholine is the neurotransmitter of the vestibular efferent system, which innervates type II HCs and both types, boutons and calyces, of afferent endings (Ishiyama et al., 1994; Lysakowski and Goldberg, 1997; Simmons et al., 2011; Schneider et al., 2021). Therefore, our data suggest that chronic ototoxicity modifies the sensitivity of the afferent terminals to the efferent input. Interestingly, a recent review suggests that the efferent system is not involved in short-term afferent coding, but in long-term regulation of afferent responsiveness (Cullen and Wei, 2021). In any case, the present results indicate that the response of the vestibular ganglion neurons to subchronic IDPN ototoxicity includes a global modification in the strength of their three synaptic contacts, those with the HCs, those with the efferent system, and those with the postsynaptic neurons in the central nervous system.

Taken together, the present data reveal that chronic ototoxic exposure (at least in the IDPN model) induces in the vestibular ganglion

neurons a response of downregulation of genes involved in synaptic function, neuronal activity, and synaptic plasticity. Abundant literature data support the conclusion that this is a response of the neurons to deafferentation and/or trophic input. As such, expression of the vesicular glutamate transporter (*Slc17a2*) gene, one of the major downregulated synaptic genes, has been associated with neuronal activity (Doyle et al., 2010), as has the expression of *Camk1g* (Harrill et al., 2010) and *Nptx2* (Xu et al., 2003; Doyle et al., 2010). Upregulation of *Nptx2* in dorsal root ganglion neurons has been recently shown to be a key step in the facilitation of synaptic input onto spinal neurons in a model of chronic itch (Kanehisa et al., 2022), so the recorded decrease in *Nptx2* expression is likely associated with reduced efficiency of the central synapses of the ganglion neurons. Potentially related result are the decreased expression of *Fgf12*, a modulator of neuronal excitability (Liu et al., 2003; Goldfarb et al., 2007) known to be expressed in vestibular ganglion neurons (Hanada et al., 2018), and the downregulation of transcription factors and receptors that promote neurite growth and differentiation, *Etv5* (Fontanet et al., 2013; Fontanet et al., 2016), *Gpr3* (Tanaka et al., 2022; Masuda et al., 2022), and *Etv4* (Fontanet et al., 2016). Interestingly, *Etv5* is well known for its role in regulating sub-synaptic gene expression in skeletal muscles (Hippenmeyer et al., 2007), so it may have a mediating role in the observed effect in genes of the proteins in cholinergic synapses. Finally, we noticed that the expression of several of these genes (*Camk1g*, *Slc17a6*, *Etv4*, *Etv5*, *Nptx2*) and other DEGs (*Ngfr*, *Vgf*) is known to be controlled by BDNF and mediate neurotrophin-induced changes in synaptic strength (Alder et al., 2003; Takemoto-Kimura et al., 2007; Melo et al., 2013; Fontanet et al., 2016; Liu et al., 2016; Mariga et al., 2015). For that reason, we evaluated the expression of *Bdnf* in the sensory epithelium and observed a strong decrease in the mRNA levels of this neurotrophin. Therefore, loss of the activity-dependent release of BDNF in the vestibular epithelium (Chabbert et al., 2003) may trigger at least part of the observed gene expression response in the ganglion. This hypothesis agrees with previous transcriptomic data. BDNF has been shown to predominantly regulate the expression of genes related to synaptic function in striatal neurons in culture (Koshimizu et al., 2021). In another study, disruption of BDNF-TrkB signalling in cortical cortistatin interneurons has been found to modify the expression of genes important for excitatory neuron function (Maynard et al., 2020). A related hypothesis is that the gene expression response identified here may represent a first step, still reversible, towards neuronal degeneration. This is a plausible hypothesis, given the known requirement of BDNF signalling for the survival of vestibular ganglion neurons (Sciarretta et al., 2010; Elliott et al., 2021), and the overall survival of the neurons at the time of our histological examination. For future studies, we hypothesize that enhancing BDNF signalling may not only increase the long-term survival of deafferented vestibular ganglion neurons, but may also facilitate recovery of partial loss of function due to chronic ototoxicity or other chronic mild stress insults that cause synaptic uncoupling.

5. Conclusions

This study identified the gene expression response of the vestibular ganglion to subchronic IDPN ototoxicity in rodents. The results obtained show a robust decrease in expression in synaptic protein and activity-dependent genes that suggest that the ganglion neurons respond to decreased synaptic input and/or BDNF signalling by modifying the function in all their synaptic contacts, both as postsynaptic and presynaptic players.

Supplementary data to this article can be found online at https://doi.org/10.1016/j.nbd.2023.106134.

Funding

This work was supported by Ministerio de Ciencia e Innovación, Agencia Estatal de Investigación, MCIU/AEI, 10.13039/501100011033, and European Regional Development Fund, FEDER [grant numbers RTI2018-096452-B-I00 and PID2021-124678OB-100], the MCIU/AEI, 10.13039/501100011033, NextGenerationEU/PRTR, ERANET NEURON Program VELOSO [grant number PCI2020-120681-2] and Agència de Gestió d'Ajuts Universitaris i de Recerca, AGAUR, Generalitat de Catalunya [grant number 2017SGR621]. A.E.C. is funded by ISCIII /MINECO and co-funded by FEDER [grant number PT17/0009/0019]. A.B.G is a Serra-Húnter fellow (Generalitat de Catalunya). E.A.G. and M.B. were supported by the Formación del Profesorado Universitario (FPU) program (Ministerio de Universidades).

CRediT authorship contribution statement

Erin A. Greguske: Investigation, Formal analysis, Writing – review & editing. **Alberto F. Maroto:** Investigation, Formal analysis, Writing – review & editing. **Mireia Borrajo:** Investigation, Formal analysis, Writing – review & editing. **Aïda Palou:** Investigation, Formal analysis, Writing – review & editing. **Marta Gut:** Methodology, Resources, Writing – original draft, Supervision. **Anna Esteve-Codina:** Formal analysis, Data curation, Writing – original draft. **Alejandro Barrallo-Gimeno:** Formal analysis, Visualization, Writing – review & editing, Funding acquisition. **Jordi Llorens:** Conceptualization, Investigation, Methodology, Formal analysis, Writing – original draft, Supervision, Project administration, Funding acquisition.

Declaration of Competing Interest

The authors declare no competing interests.

Data availability

The RNAseq data are available from the GEO repository. The accession number and appropriate link are provided in the manuscript.

Acknowledgements

The confocal microscopy studies were performed at the Centres Científics i Tecnològics de la UB (CCiTUB) of the Universitat de Barcelona. We thank Dr. Benjamín Torrejon-Escribano for his expert and technical help. We also thank student Clara López for her contribution towards the immunohistochemical studies and Dr. Mireia Martín-Satué for her guidance with the RNA-scope analysis.

References

Alder, J., Thakker-Varia, S., Bangasser, D.A., Kuroiwa, M., Plummer, M.R., Shors, T.J., Black, I.B., 2003. Brain-derived neurotrophic factor-induced gene expression reveals novel actions of VGF in hippocampal synaptic plasticity. J. Neurosci. 23 (34), 10800–10808. https://doi.org/10.1523/JNEUROSCI.23-34-10800.2003.

Ashburner, M., Ball, C.A., Blake, J.A., Botstein, D., Butler, H., Cherry, J.M., Davis, A.P., Dolinski, K., Dwight, S.S., Eppig, J.T., Harris, M.A., Hill, D.P., Issel-Tarver, L., Kasarskis, A., Lewis, S., Matese, J.C., Richardson, J.E., Ringwald, M., Rubin, G.M., Sherlock, G., 2000. Gene ontology: tool for the unification of biology. Gene Ontol. Consortium. Nat. Genet. 25, 25–29. https://doi.org/10.1038/75556.

Bacqué-Cazenave, J., Courtand, G., Beraneck, M., Straka, H., Combes, D., Lambert, F.M., 2022. Locomotion-induced ocular motor behavior in larval Xenopus is developmentally tuned by visuo-vestibular reflexes. Nat. Commun. 13, 2957. https://doi.org/10.1038/s41467-022-30636-6.

Balbuena, E., Llorens, J., 2001. Behavioural disturbances and sensory pathology following allylnitrile exposure in rats. Brain Res. 904, 298–306. https://doi.org/10.1016/s0006-8993(01)02476-3.

Balbuena, E., Llorens, J., 2003. Comparison of cis- and trans-crotononitrile effects in the rat reveals specificity in the neurotoxic properties of nitrile isomers. Toxicol. Appl. Pharmacol. 187, 89–100. https://doi.org/10.1016/s0041-008x(02)00039-x.

Black, F.O., Gianna-Poulin, C., Pesznecker, S.C., 2001. Recovery from vestibular ototoxicity. Otol. Neurotol. 22, 662–671.

Boadas-Vaello, P., Riera, J., Llorens, J., 2005. Behavioral and pathological effects in the rat define two groups of neurotoxic nitriles. Toxicol. Sci. 88, 456–466. https://doi.org/10.1093/toxsci/kfi314.

Boadas-Vaello, P., Sedó-Cabezón, L., Verdú, E., Llorens, J., 2017. Strain and sex differences in the vestibular and systemic toxicity of 3,3′-iminodipropionitrile in mice. Toxicol. Sci. 156, 109–122. https://doi.org/10.1093/toxsci/kfw238.

Burns, J.C., Stone, J.S., 2017. Development and regeneration of vestibular hair cells in mammals. Sem. Cell Develop. Biol. 65, 96–105. https://doi.org/10.1016/j.semcdb.2016.11.001.

Cassel, R., Bordiga, P., Carcaud, J., Simon, F., Beraneck, M., Le Gall, A., Benoit, A., Bouet, V., Philoxene, B., Besnard, S., Watabe, I., Pericat, D., Hautefort, C., Assie, A., Tonetto, A., Dyhrfjeld-Johnsen, J., Llorens, J., Tighilet, B., Chabbert, C., 2019. Morphological and functional correlates of vestibular synaptic deafferentation and repair in a mouse model of acute-onset vertigo. Dis. Model. Mech. 12, dmm039115. https://doi.org/10.1242/dmm.039115.

Chabbert, C., Mechaly, I., Sieso, V., Giraud, P., Brugeaud, A., Lehouelleur, J., Couraud, F., Valmier, J., Sans, A., 2003. Voltage-gated Na+ channel activation induces both action potentials in utricular hair cells and brain-derived neurotrophic factor release in the rat utricle during a restricted period of development. J. Physiol. 553, 113–123. https://doi.org/10.1113/jphysiol.2003.043034.

Chen, E.Y., Tan, C.M., Kou, Y., Duan, Q., Wang, Z., Meirelles, G.V., Clark, N.R., Ma'ayan, A., 2013. Enrichr: interactive and collaborative HTML5 gene list enrichment analysis tool. BMC Bioinform. 14, 128. https://doi.org/10.1186/1471-2105-14-128.

Chou, S.M., Hartmann, H.A., 1964. Axonal lesions and waltzing syndrome after idpn administration in rats. With a concept–"axostasis". Acta Neuropathol. 3, 428–450. https://doi.org/10.1007/BF00688453.

Cullen, K.E., Wei, R.H., 2021. Differences in the structure and function of the vestibular ffferent system among vertebrates. Front. Neurosci. 15, 684800 https://doi.org/10.3389/fnins.2021.684800.

Dobin, A., Davis, C.A., Schlesinger, F., Drenkow, J., Zaleski, C., Jha, S., Batut, P., Chaisson, M., Gingeras, T.R., 2013. STAR: ultrafast universal RNA-seq aligner. Bioinformatics. 29, 15–21. https://doi.org/10.1093/bioinformatics/bts635.

Doyle, S., Pyndiah, S., De Gois, S., Erickson, J.D., 2010. Excitation-transcription coupling via calcium/calmodulin-dependent protein kinase/ERK1/2 signaling mediates the coordinate induction of VGLUT2 and Narp triggered by a prolonged increase in glutamatergic synaptic activity. J. Biol. Chem. 285, 14366–14376. https://doi.org/10.1074/jbc.M109.080069.

Elliott, K.L., Straka, K., 2022. Assembly and functional organization of the vestibular system. In: Evolution of Neurosensory Cells and Systems. CRC Press, pp. 135–174.

Elliott, K.L., Kersigo, J., Lee, J.H., Yamoah, E.N., Fritzsch, B., 2021. Sustained loss of Bdnf affects peripheral but not central vestibular targets. Front. Neurol. 12, 768456 https://doi.org/10.3389/fneur.2021.768456.

Fariñas, I., Jones, K.R., Tessarollo, L., Vigers, A.J., Huang, E., Kirstein, M., de Caprona, D. C., Coppola, V., Backus, C., Reichardt, L.F., Fritzsch, B., 2001. Spatial shaping of cochlear innervation by temporally regulated neurotrophin expression. J. Neurosci. 21, 6170–6180. https://doi.org/10.1523/JNEUROSCI.21-16-06170.2001.

Fontanet, P., Irala, D., Alsina, F.C., Paratcha, G., Ledda, F., 2013. Pea3 transcription factor family members Etv4 and Etv5 mediate retrograde signaling and axonal growth of DRG sensory neurons in response to NGF. J. Neurosci. 33, 15940–15951. https://doi.org/10.1523/JNEUROSCI.0928-13.2013.

Fontanet, P.A., Ríos, A.S., Alsina, F.C., Paratcha, G., Ledda, F., 2016. Pea3 transcription factors, Etv4 and Etv5, are required for proper hippocampal dendrite development and plasticity. Cereb. Cortex 28, 236–249. https://doi.org/10.1093/cercor/bhw372.

Fritzsch, B., Barbacid, M., Silos-Santiago, I., 1998. The combined effects of trkB and trkC mutations on the innervation of the inner ear. Int. J. Dev. Neurosci. 16, 493–505. https://doi.org/10.1016/s0736-5748(98)00043-4.

Fritzsch, B., Tessarollo, L., Coppola, E., Reichardt, L.F., 2004. Neurotrophins in the ear: their roles in sensory neuron survival and fiber guidance. Prog. Brain Res. 146, 265–278. https://doi.org/10.1016/S0079-6123(03)46017-2.

Fritzsch, B., Kersigo, J., Yang, T., Jahan, I., Pan, N., 2016. Neurotrophic factor function during ear development: Expression changes define critical phases for neuronal viability. In: Dabdoub, A., Fritzsch, B., Popper, A., Fay, R. (Eds.), The Primary Auditory Neurons of the Mammalian Cochlea. Springer Handbook of Auditory Research, vol. 52. Springer, New York, NY. https://doi.org/10.1007/978-1-4939-3031-9_3.

Gaboyard-Niay, S., Travo, C., Saleur, A., Broussy, A., Brugeaud, A., Chabbert, C., 2016. Correlation between afferent rearrangements and behavioral deficits after local excitotoxic insult in the mammalian vestibule: a rat model of vertigo symptoms. Dis. Model. Mech. 9, 1181–1192. https://doi.org/10.1242/dmm.024521.

Gene Ontology Consortium, 2021. The gene ontology resource: enriching a GOld mine. Nucleic Acids Res. 49 (D1), D325–D334. https://doi.org/10.1093/nar/gkaa1113.

Goldfarb, M., Schoorlemmer, J., Williams, A., Diwakar, S., Wang, Q., Huang, X., Giza, J., Tchetchik, D., Kelley, K., Vega, A., Matthews, G., Rossi, P., Ornitz, D.M., D'Angelo, E., 2007. Fibroblast growth factor homologous factors control neuronal excitability through modulation of voltage-gated sodium channels. Neuron 55, 449–463. https://doi.org/10.1016/j.neuron.2007.07.006.

Greguske, E.A., Carreres-Pons, M., Cutillas, B., Boadas-Vaello, P., Llorens, J., 2019. Calyx junction dismantlement and synaptic uncoupling precede hair cell extrusion in the vestibular sensory epithelium during sub-chronic 3,3′-iminodipropionitrile ototoxicity in the mouse. Arch. Toxicol. 93, 417–434.

Griffin, J.W., Hoffman, P.N., Clark, A.W., Carroll, P.T., Price, D.L., 1978. Slow axonal transport of neurofilament proteins: impairment of beta,beta'-iminodipropionitrile administration. Science 202, 633–635. https://doi.org/10.1126/science.81524.

Greguske, E.A., Llorens, J., Pyott, S.J., 2021. Assessment of cochlear toxicity in response to chronic 3,3'-iminodipropionitrile in mice reveals early and reversible functional loss that precedes overt histopathology. Archives of toxicology 95 (3), 1003–1021. https://doi.org/10.1007/s00204-020-02962-5.

Griffin, J.W., Drucker, N., Gold, B.G., Rosenfeld, J., Benzaquen, M., Charnas, L.R., Fahnestock, K.E., Stocks, E.A., 1987. Schwann cell proliferation and migration during paranodal demyelination. J. Neurosci. 7, 682–699. https://doi.org/10.1523/JNEUROSCI.07-03-00682.1987.

Hanada, Y., Nakamura, Y., Ozono, Y., Ishida, Y., Takimoto, Y., Taniguchi, M., Ohata, K., Koyama, Y., Imai, T., Morihana, T., Kondo, M., Sato, T., Inohara, H., Shimada, S., 2018. Fibroblast growth factor 12 is expressed in spiral and vestibular ganglia and necessary for auditory and equilibrium function. Sci. Report. 8, 11491. https://doi.org/10.1038/s41598-018-28618-0.

Harrill, J.A., Knapp, G.W., Crofton, K.M., 2010. Splice variant specific increase in Ca2+/calmodulin-dependent protein kinase 1-gamma mRNA expression in response to acute pyrethroid exposure. J. Biochem. Mol. Toxicol. 24, 174–186. https://doi.org/10.1002/jbt.20324.

Hippenmeyer, S., Huber, R.M., Ladle, D.R., Murphy, K., Arber, S., 2007. ETS transcription factor Erm controls subsynaptic gene expression in skeletal muscles. Neuron 55, 726–740. https://doi.org/10.1016/j.neuron.2007.07.028.

Ishiyama, A., Lopez, I., Wackym, P.A., 1994. Choline acetyltransferase immunoreactivity in the human vestibular end-organs. Cell Biol. Int. 18, 979–984. https://doi.org/10.1006/cbir.1994.1019.

The vestibular system. In: Kandel, E.R., Koester, J.D., Mack, S.H., Siegelbaum, S.A. (Eds.), 2021. In: Principles of Neural Science, 6e. Hill, McGraw.

Kanehisa, M., Goto, S., 2000. KEGG: Kyoto encyclopedia of genes and genomes. Nucleic Acids Res. 28, 27–30. https://doi.org/10.1093/nar/28.1.27.

Kanehisa, K., Koga, K., Maejima, S., Shiraishi, Y., Asai, K., Shiratori-Hayashi, M., Xiao, M. F., Sakamoto, H., Worley, P.F., Tsuda, M., 2022. Neuronal pentraxin 2 is required for facilitating excitatory synaptic inputs onto spinal neurons involved in pruriceptive transmission in a model of chronic itch. Nat. Commun. 13, 2367. https://doi.org/10.1038/s41467-022-30089-x.

Kenyon, E.J., Kirkwood, N.K., Kitcher, S.R., Goodyear, R.J., Derudas, M., Cantillon, D.M., Baxendale, S., de la Vega de León, A., Mahieu, V.N., Osgood, R.T., Wilson, C.D., Bull, J.C., Waddell, S.J., Whitfield, T.T., Ward, S.E., Kros, C.J., Richardson, G.P., 2021. Identification of a series of hair-cell MET channel blockers that protect against aminoglycoside-induced ototoxicity. JCI Insight 6, e145704. https://doi.org/10.1172/jci.insight.145704.

Kersigo, J., Pan, N., Lederman, J.D., Chatterjee, S., Abel, T., Pavlinkova, G., Silos-Santiago, I., Fritzsch, B., 2018. A RNAscope whole mount approach that can be combined with immunofluorescence to quantify differential distribution of mRNA. Cell Tissue Res. 374, 251–262. https://doi.org/10.1007/s00441-018-2864-4.

Kim, G.S., Wang, T., Sayyid, Z.N., Fuhriman, J., Jones, S.M., Cheng, A.G., 2022. Repair of surviving hair cells in the damaged mouse utricle. Proc. Natl. Acad. Sci. U. S. A. 119, e2116973119 https://doi.org/10.1073/pnas.2116973119.

Koshimizu, H., Matsuoka, H., Nakajima, Y., Kawai, A., Ono, J., Ohta, K.I., Miki, T., Sunagawa, M., Adachi, N., Suzuki, S., 2021. Brain-derived neurotrophic factor predominantly regulates the expression of synapse-related genes in the striatum: insights from in vitro transcriptomics. Neuropsychopharmacol. Rep. 41, 485–495. https://doi.org/10.1002/npr2.12208.

Kuleshov, M.V., Jones, M.R., Rouillard, A.D., Fernandez, N.F., Duan, Q., Wang, Z., Koplev, S., Jenkins, S.L., Jagodnik, K.M., Lachmann, A., McDermott, M.G., Monteiro, C.D., Gundersen, G.W., Ma'ayan, A., 2016. Enrichr: a comprehensive gene set enrichment analysis web server 2016 update. Nucleic Acids Res. gkw377 https://doi.org/10.1093/nar/gkw377.

Li, B., Dewey, C.N., 2011. RSEM: accurate transcript quantification from RNA-Seq data with or without a reference genome. BMC Bioinform. 12, 323. https://doi.org/10.1186/1471-2105-12-323.

Liberman, M.C., Kujawa, S.G., 2017. Cochlear synaptopathy in acquired sensorineural hearing loss: manifestations and mechanisms. Hear. Res. 349, 138–147. https://doi.org/10.1016/j.heares.2017.01.003.

Liu, C.J., Dib-Hajj, S.D., Renganathan, M., Cummins, T.R., Waxman, S.G., 2003. Modulation of the cardiac sodium channel Nav1.5 by fibroblast growth factor homologous factor 1B. J. Biol. Chem. 278, 1029–1036. https://doi.org/10.1074/jbc.M207074200.

Liu, D., Liu, Z., Liu, H., Li, H., Pan, X., Li, Z., 2016. Brain-derived neurotrophic factor promotes vesicular glutamate transporter 3 expression and neurite outgrowth of dorsal root ganglion neurons through the activation of the transcription factors Etv4 and Etv5. Brain Res. Bull. 121, 215–226. https://doi.org/10.1016/j.brainresbull.2016.02.010.

Llorens, J., Demêmes, D., 1994. Hair cell degeneration resulting from 3,3′-iminodipropionitrile toxicity in the rat vestibular epithelia. Hear. Res. 76, 78–86. https://doi.org/10.1016/0378-5955(94)90090-6.

Llorens, J., Demêmes, D., 1996. 3,3'-Iminodipropionitrile induces neurofilament accumulations in the perikarya of rat vestibular ganglion neurons. Brain Res. 717, 118–126. https://doi.org/10.1016/0006-8993(96)00034-0.

Llorens, J., Rodríguez-Farré, E., 1997. Comparison of behavioral, vestibular, and axonal effects of subchronic IDPN in the rat. Neurotoxicol. Teratol. 19, 117–127. https://doi.org/10.1016/s0892-0362(96)00216-4.

Llorens, J., Demêmes, D., Sans, A., 1993. The behavioral syndrome caused by 3,3′-iminodipropionitrile and related nitriles in the rat is associated with degeneration of the vestibular sensory hair cells. Toxicol. Appl. Pharmacol. 123, 199–210.

Love, M.I., Huber, W., Anders, S., 2014. Moderated estimation of fold change and dispersion for RNA-seq data with DESeq2. Genome Biol. 15, 550. https://doi.org/10.1186/s13059-014-0550-8.

Lysakowski, A., Goldberg, J.M., 1997. A regional ultrastructural analysis of the cellular and synaptic architecture in the chinchilla cristae ampullares. J. Comp. Neurol. 389, 419–443. https://doi.org/10.1002/(sici)1096-9861(19971222)389:3<419::aid-cne5>3.0.co;2-3.

Mariga, A., Glaser, J., Mathias, L., Xu, D., Xiao, M., Worley, P., Ninan, I., Chao, M.V., 2015. Definition of a bidirectional activity-dependent pathway involving BDNF and Narp. Cell Rep. 13, 1747–1756. https://doi.org/10.1016/j.celrep.2015.10.064.

Maroto, A.F., Barrallo-Gimeno, A., Llorens, J., 2021a. Relationship between vestibular hair cell loss and deficits in two anti-gravity reflexes in the rat. Hear. Res. 410, 108336 https://doi.org/10.1016/j.heares.2021.108336.

Maroto, A.F., Greguske, E.A., Deulofeu, M., Boadas-Vaello, P., Llorens, J., 2021b. Behavioral assessment of vestibular dysfunction in rats. In: Llorens, J., Barenys, M. (Eds.), Experimental Neurotoxicology Methods, Neuromethods, vol. 172. Springer US, pp. 199–215.

Maroto, A.F., Borrajo, M., Prades, S., Callejo, À., Amilibia, E., Pérez-Grau, M., Roca-Ribas, F., Castellanos, E., Barrallo-Gimeno, A., Llorens, J., 2022. The vestibular calyceal junction is dismantled following subchronic streptomycin in rats and sensory epithelium stress in humans. BioRxiv Manuscript. https://doi.org/10.1101/2022.05.17.492294.

Martins-Lopes, V., Bellmunt, A., Greguske, E.A., Maroto, A.F., Boadas-Vaello, P., Llorens, J., 2019. Quantitative assessment of anti-gravity reflexes to evaluate vestibular dysfunction in rats. J. Assoc. Res. Otolaryngol. 20, 553–563.

Masuda, S., Tanaka, S., Shiraki, H., Sotomaru, Y., Harada, K., Hide, I., Kiuchi, Y., Sakai, N., 2022. GPR3 expression in retinal ganglion cells contributes to neuron survival and accelerates axonal regeneration after optic nerve crush in mice. Neurobiol. Dis. 172, 105811 https://doi.org/10.1016/j.nbd.2022.105811.

Maynard, K.R., Kardian, A., Hill, J.L., Mai, Y., Barry, B., Hallock, H.L., Jaffe, A.E., Martinowich, K., 2020. TrkB signaling influences gene expression in cortistatin-expressing interneurons. eNeuro 7 (1). https://doi.org/10.1523/ENEURO.0310-19.2019. ENEURO.0310-19.2019.

Melo, C.V., Mele, M., Curcio, M., Comprido, D., Silva, C.G., Duarte, C.B., 2013. BDNF regulates the expression and distribution of vesicular glutamate transporters in cultured hippocampal neurons. PLoS One 8, e53793. https://doi.org/10.1371/journal.pone.0053793.

Mootha, V.K., Lindgren, C.M., Eriksson, K.F., Subramanian, A., Sihag, S., Lehar, J., Puigserver, P., Carlsson, E., Ridderstråle, M., Laurila, E., Houstis, N., Daly, M.J., Patterson, N., Mesirov, J.P., Golub, T.R., Tamayo, P., Spiegelman, B., Lander, E.S., Hirschhorn, J.N., Altshuler, D., Groop, L.C., 2003. PGC-1alpha-responsive genes involved in oxidative phosphorylation are coordinately downregulated in human diabetes. Nat. Genet. 34, 267–273. https://doi.org/10.1038/ng1180.

O'Sullivan, M.E., Perez, A., Lin, R., Sajjadi, A., Ricci, A.J., Cheng, A.G., 2017. Towards the prevention of aminoglycoside-related hearing loss. Front. Cell. Neurosci. 11, 325. https://doi.org/10.3389/fncel.2017.00325.

Picelli, S., Faridani, O.R., Björklund, A.K., Winberg, G., Sagasser, S., Sandberg, R., 2014. Full-length RNA-seq from single cells using smart-seq2. Nat. Protoc. 9, 171–181. https://doi.org/10.1038/nprot.2014.006.

Reijntjes, D., Breitzler, J.L., Persic, D., Pyott, S.J., 2021. Preparation of the intact rodent organ of Corti for RNAscope and immunolabeling, confocal microscopy, and quantitative analysis. STAR Protoc. 2, 100544 https://doi.org/10.1016/j.xpro.2021.100544.

Saldaña-Ruíz, S., Boadas-Vaello, P., Sedó-Cabezón, L., Llorens, J., 2013. Reduced systemic toxicity and preserved vestibular toxicity following co-treatment with nitriles and CYP2E1 inhibitors: a mouse model for hair cell loss. J. Assoc. Res. Otolaryngol. 14, 661–671.

Schneider, G.T., Lee, C., Sinha, A.K., Jordan, P.M., Holt, J.C., 2021. The mammalian efferent vestibular system utilizes cholinergic mechanisms to excite primary vestibular afferents. Sci. Rep. 11, 1231. https://doi.org/10.1038/s41598-020-80367-1.

Sciarretta, C., Fritzsch, B., Beisel, K., Rocha-Sanchez, S.M., Buniello, A., Horn, J.M., Minichiello, L., 2010. PLCγ-activated signalling is essential for TrkB mediated sensory neuron structural plasticity. BMC Dev. Biol. 10, 103. https://doi.org/10.1186/1471-213X-10-103.

Sedó-Cabezón, L., Jedynak, P., Boadas-Vaello, P., Llorens, J., 2015. Transient alteration of the vestibular calyceal junction and synapse in response to chronic ototoxic insult in rats. Dis. Model. Mech. 8, 1323–1337.

Seoane, A., Demêmes, D., Llorens, J., 2001. Relationship between insult intensity and mode of hair cell loss in the vestibular system of rats exposed to 3,3′-iminodipropionitrile. J. Comp. Neurol. 439, 385–399. https://doi.org/10.1002/cne.1357.

Seoane, A., Demêmes, D., Llorens, J., 2003. Distal effects in a model of proximal axonopathy: 3,3′-iminodipropionitrile causes specific loss of neurofilaments in rat vestibular afferent endings. Acta Neuropathol. 106, 458–470. https://doi.org/10.1007/s00401-003-0744-8.

Simmons, D., Duncan, J., de Caprona, D.C., Fritzsch, B., 2011. Development of the inner ear efferent system. In: Ryugo, D., Fay, R. (Eds.), Auditory and Vestibular Efferents. Springer Handbook of Auditory Research, vol. 38. Springer, New York, NY. https://doi.org/10.1007/978-1-4419-7070-1_7.

Soler-Martín, C., Díez-Padrisa, N., Boadas-Vaello, P., Llorens, J., 2007. Behavioral disturbances and hair cell loss in the inner ear following nitrile exposure in mice, guinea pigs and frogs. Toxicol. Sci. 96, 123–132.

Soler-Martín, C., Boadas-Vaello, P., Saldaña-Ruíz, S., Cutillas, B., Llorens, J., 2011. Butenenitriles have low axonopathic potential in the rat. Toxicol. Lett. 200, 187–193. https://doi.org/10.1016/j.toxlet.2010.11.014.

Steyger, P.S., 2021. Mechanisms of aminoglycoside- and cisplatin-induced ototoxicity. Amer. J. Audiol. 30 (3S), 887–900. https://doi.org/10.1044/2021_AJA-21-00006.

Subramanian, A., Tamayo, P., Mootha, V.K., Mukherjee, S., Ebert, B.L., Gillette, M.A., Paulovich, A., Pomeroy, S.L., Golub, T.R., Lander, E.S., Mesirov, J.P., 2005. Gene set enrichment analysis: a knowledge-based approach for interpreting genome-wide expression profiles. Proc. Natl. Acad. Sci. U. S. A. 102 (43), 15545–15550. https://doi.org/10.1073/pnas.0506580102.

Sultemeier, D.R., Hoffman, L.F., 2017. Partial aminoglycoside lesions in vestibular epithelia reveal broad sensory dysfunction associated with modest hair cell loss and afferent calyx retraction. Front. Cell. Neurosci. 11, 331.

Takemoto-Kimura, S., Ageta-Ishihara, N., Nonaka, M., Adachi-Morishima, A., Mano, T., Okamura, M., Fujii, H., Fuse, T., Hoshino, M., Suzuki, S., Kojima, M., Mishina, M., Okuno, H., Bito, H., 2007. Regulation of dendritogenesis via a lipid-raft-associated Ca2+/calmodulin-dependent protein kinase CLICK-III/CaMKIgamma. Neuron 54 (5), 755–770. https://doi.org/10.1016/j.neuron.2007.05.021.

Tanaka, S., Shimada, N., Shiraki, H., Miyagi, T., Harada, K., Hide, I., Sakai, N., 2022. GPR3 accelerates neurite outgrowth and neuronal polarity formation via PI3 kinase-mediating signaling pathway in cultured primary neurons. Mol. Cell. Neurosci. 118, 103691 https://doi.org/10.1016/j.mcn.2021.103691.

Wang, G.P., Basu, I., Beyer, L.A., Wong, H.T., Swiderski, D.L., Gong, S.S., Raphael, Y., 2017. Severe streptomycin ototoxicity in the mouse utricle leads to a flat epithelium but the peripheral neural degeneration is delayed. Hear. Res. 355, 33–41.

Xie, Z., Bailey, A., Kuleshov, M.V., Clarke, D., Evangelista, J.E., Jenkins, S.L., Lachmann, A., Wojciechowicz, M.L., Kropiwnicki, E., Jagodnik, K.M., Jeon, M., Ma'ayan, A., 2021. Gene set knowledge discovery with Enrichr. Curr. Protoc. 1, e90 https://doi.org/10.1002/cpz1.90.

Xu, D., Hopf, C., Reddy, R., Cho, R.W., Guo, L., Lanahan, A., Petralia, R.S., Wenthold, R. J., O'Brien, R.J., Worley, P., 2003. Narp and NP1 form heterocomplexes that function in developmental and activity-dependent synaptic plasticity. Neuron 39, 513–528. https://doi.org/10.1016/s0896-6273(03)00463-x.